Modeling the Assembly of Compliant, Non-ideal Parts

by

Minho Chang

S.M., Mechanical Engineering
Massachusetts of Institute of Technology, 1993

B.S., Mechanical Design and Production Engineering
Seoul National University, 1991

Submitted to the Department of Mechanical Engineering
in Partial Fulfillment of the Requirements for the Degree of
Doctor of Philosophy in Mechanical Engineering

at the

Massachusetts Institute of Technology

February 1996

Signature of Author_____
Department of Mechanical Engineering
December 19, 1995

Certified by_____
Professor David C. Gossard

Accepted by_____
Professor Ain A. Sonin
Chairman, Department Committee

Modeling the Assembly of Compliant, Non-ideal Parts

by
MINHO CHANG

Submitted to the Department of Mechanical Engineering
on December 22, 1995
in Partial Fulfillment of the Requirements
for the Degree of Doctor of Philosophy in
Mechanical Engineering

Abstract

All manufactured parts and tooling have unavoidable variations from their nominal shape. During assembly, compliant parts are further deformed by the relatively-rigid tooling. Lack of knowledge regarding variations and deformation often results in expensive "fit-up" problems. For example, manufactured parts can not be fit together during the assembly process, or variations in the final product are out of specification. Required time and cost for engineering change increase exponentially as the product development process evolves. By the time parts and tooling are manufactured, the cost of scrapped, reworked or delayed assemblies become considerable.

Since most current computer-aided design (CAD) systems are based on ideally-sized and ideally-located rigid geometry, they are unable to model or predict the effects of variations in parts and tooling in assemblies of compliant parts, e.g. automobile body assembly. Within this context, a computational framework for the rational treatment of deformations and variations in parts and tooling forms an important foundation for more effective CAD systems in the future.

This thesis proposes a conceptual framework for modeling and simulating the assembly of compliant, non-ideal parts for future CAD systems. Several new concepts are proposed to represent parts, assembly tooling, and assembly processes in CAD systems: notably *PCFR cycle* and *contact chain*. Procedures are developed to simulate propagation of variations in complex assembly processes. The results of the simulation enable us to

- identify critical dimensions in both parts and assembly tooling,
- predict potential variation-related assembly problems before they occur,
- trace existing problems back to their root cause(s), and
- evaluate the degree to which a given design of product, tooling, and assembly process is robust to variations in incoming parts.

Thesis Supervisor: David C. Gossard
Title: Professor of Mechanical Engineering

Acknowledgments

I would like to thank my advisor, David Gossard, for his constant guidance and support of all conceivable sorts.

I also like to express my appreciation to all of my friends in the MIT cadlab and the Agile manufacturing program for their comments and suggestions.

Thanks go to Stephen, Naren, and Krish for proof reading my thesis.

Much appreciation to Applicon and U.S. Airforce for their financial support.

Thanks go to my former advisor, Kunwoo Lee, for having introduced me in this field of research and for his continuous encouragement.

Special thanks go to my parents, Jinho, Inji, and especially Sujin for being so understanding during this work.

Table of Contents

Abstract 2

Acknowledgment 3

Table of Contents 4

Table of Figures 8

Table of Tables 10

Chapter 1. Introduction 11

1.1. Motivation 11

1.2. Sources of variation-related assembly problems 12

1.2.1. Parts are designed incorrectly 14

1.2.2. Parts are manufactured incorrectly 14

1.2.3. Parts are assembled incorrectly 15

1.3. Problem statements and goals 15

1.4. Overview of thesis 16

Chapter 2. Related Work 18

2.1. Interpretation of variations in parts 18

2.1.1. Parameter space approach 18

2.1.2. True positioning approach 19

2.1.3. Discussion 19

2.2. Assembly modeling 19

2.2.1. Assembly model of ideal parts 20

2.2.2. Assembly model of non-ideal parts 20

2.2.3. Discussion 21

2.3. Tolerance analysis and synthesis 21

2.3.1. Worst case versus root sum square 22

2.3.2. Discussion 23

2.4. Diagnosis of variation-related assembly problems 23
2.4.1. Diagnosis of automobile body assembly 24
2.4.2. Discussion 25
Chapter 3. Representation 26
3.1. Nomenclature 26
3.2. Components 28
3.2.1. Geometry 28
3.2.2. Features 28
3.2.3. Graph representation 29
3.3. Mating features 30
3.4. Variations 32
3.5. Force, displacement, and constitutive relations 36
3.6. Summary 37
Chapter 4. Assembly Modeling 39
4.1. Unit of assembly process: PCFR cycle 39
4.2. Graph representation of PCFR cycles: Contact chain 43
4.3. Overview of simulation 45
4.4. Procedure 1: Finding deviation of welding spots 47
4.5. Procedure 2: Finding variations in the assembly 51
4.6. Simulation of multiple PCFR cycles 53
4.7. Summary 55
Chapter 5. Validation 56
5.1. Example 1. Assembly with one weld joint 58
5.1.1. Effects of variations in parts 59
5.1.2. Effects of variations in locator pins 62
5.1.3. Effects of variations in locator blocks/clamps 64
5.1.4. Effects of variations in welding guns 65

5.2. Example 2. Assembly with two weld joints 66
5.3. Example 3. Assembly through multiple PCFR cycles 69
5.4. Summary 71
Chapter 6. Applications 73
6.1. Identification of process monitoring points 73
6.1.1. The assembly 74
6.1.2. Measuring points 75
6.1.3. Mating features 75
6.1.4. Identified critical dimensions and their sensitivities 76
6.2. Evaluation of robustness of design 78
6.3. Diagnosis of assembly problems 80
6.3.1. Diagnostic problem solving process 81
6.3.2. Inherent difficulties of diagnosis 81
6.4. Representation of system knowledge 82
6.5. Diagnostic mechanism: for special cases 83
6.6. Diagnostic mechanism: for single a fault 84
6.7. Diagnostic mechanism: for multiple faults 85
6.7.1. Qualitative description of the approach 85
6.7.2. Quantitative criteria for plausible explanations 89
6.7.3. Further refinement of multiple-fault diagnosis 92
6.8. Validation 92
Chapter 7. Conclusion 96
7.1. Contributions 96
7.2. Recommendations 97
7.2.1. Other applications of the assembly model 97
7.2.2. Limitations and possible improvements 98
References 99

Appendix A. Homogeneous transformation matrix..... ..102

Appendix B. Coordinate transformation of variations and displacements 104

Appendix C. Shape error and position error.....105

Appendix D. Static condensation 107

Appendix E. Addition of variations and displacements 108

Table of Figures

Figure 1.1 Flow of the automobile body development process 13

Figure 1.2 Sources of variation-related assembly problems 14

Figure 3.1 Parametric representation of a surface 28

Figure 3.2 Position of a feature 29

Figure 3.3 Graph representation of a part 30

Figure 3.4 Pin/hole mate 32

Figure 3.5 Shape errors and position errors 33

Figure 3.6 3-2-1 locator scheme 34

Figure 3.7 Position error of a feature 35

Figure 4.1 Assembly process of automobile body 40

Figure 4.2 PCFR cycles 41

Figure 4.3 Graph representation of interaction between parts and tooling 44

Figure 4.4 Graph representation of the PCFR cycles 45

Figure 4.5 The closed loop of variations, displacement during assembly, and relative motion between a pair of mating features 48

Figure 4.6 Deviation of welding spots 50

Figure 4.7 Geometric compatibility at weld joint 52

Figure 4.8 Simulation of a PCFR cycle: summary 54

Figure 4.9 Simulation of multiple PCFR cycles 54

Figure 5.1 Variations in two dimensional space 56

Figure 5.2 Two dimensional assembly consisting of two parts 59

Figure 5.3 Effects of variations in parts 60

Figure 5.4 Closed-up of the welding surface of part A during fastening 61

Figure 5.5 Effects of variation in locator pins 63

Figure 5.6 Effects of variations in locator blocks/clamps 64

Figure 5.7 Effects of variations in welding guns 65

Figure 5.8 Assembly with multiple welds 67
Figure 5.9 Effects of variations when assembly has locked-up stresses.....68
Figure 5.10 Two dimensional assembly consisting of three parts 70
Figure 6.1 Front-end assembly 74
Figure 6.2 Simplified front-end assembly 74
Figure 6.3 Measuring points on the front-end assembly.....75
Figure 6.4 Mating features in the front-end assembly.....75
Figure 6.5 Critical features for the front-end assembly 76
Figure 6.6 Assembly tooling design alternatives.....78
Figure 6.7 Product design alternative: assembly with a lap joint.....79
Figure 6.8 Assembly sequence alternatives.....80
Figure 6.9 Schematic of the diagnostic problem solving process.....81
Figure 6.10 Measurement data and deviation modes 86
Figure 6.11 Measurement data and a plane constructed by two deviation modes.....88

Table of Tables

Table 2.1 Root cause - symptom relation table provided by Ceglarek et al. 24

Table 4.1 Geometric compatibility at mating features 49

Table 5.1 Geometric compatibility at two dimensional mating features 58

Table 6.1 The results of sensitivity analysis 77

Table 6.2 Measurement data 93

Table 6.3 Diagnosis results 94

1

Introduction

1.1. Motivation

Managing variations, i.e., dimensional errors, is essential to retaining competitiveness in the automotive industry because excessive variations directly affect product quality, time-to-market, and cost:

- Variations are directly related to customer satisfaction. For example, too-large or too-small gaps between the door and door aperture cause crucial problems such as high door closing effort, noise, and leakage as well as poor appearance of the vehicle.

- Variations increase product development time and cost as well. Currently about six months are dedicated for installation and tryout of tooling, when a new model is developed[1]. Major activities during this period include finding and eliminating excessive variations in the automobile body assembly. These often create a bottleneck in this launch period.

[1]This period is called as *launch* in automobile industry.

- Variations cause other expensive problems such as rework, scrap, warranty claims. Rework is a non-value adding activity that can add significant labor costs. Sometimes large quantities of parts or subassemblies are wasted because of the excessive variations. Warranty claims are even more expensive because they not only increase immediate labor costs but also detract from the company's reputation[2].

The fact that variations are critical to quality, time-to-market, and cost is not unique to the automotive industry but common in virtually any manufacturing industry. Therefore, methods to anticipate and control variation will have major positive impact.

1.2. Sources of variation-related assembly problems

The automobile body development process is roughly divided into four steps: styling, design, fabrication, and assembly. Figure 1.1 illustrates the flow of the automobile body development process. For the purpose of this thesis, styling is defined as the conceptual design of the overall shape of the visible assemblies, e.g., the surface of closure panels such as the hood, fender, or door, that customers can see. On the other hand, design refers to the design of individual parts including both closure panels and structural parts[3]. Fabrication is the manufacturing of parts, and assembly is the putting together of parts.

At each step, variations arise because of both inevitable variations in the manufacturing process and human errors. As a result, the final assembly always differs from the original design. If excessive variations occur in the dimensions that customers care about strongly, such as the margin between door and door aperture, these become critical.

---

[2]In some companies, cost for a warranty claim is estimated to be four times the cost of resolving the claim.
[3]Structural parts are located inside the closure panels, and their major function is to support the vehicle.

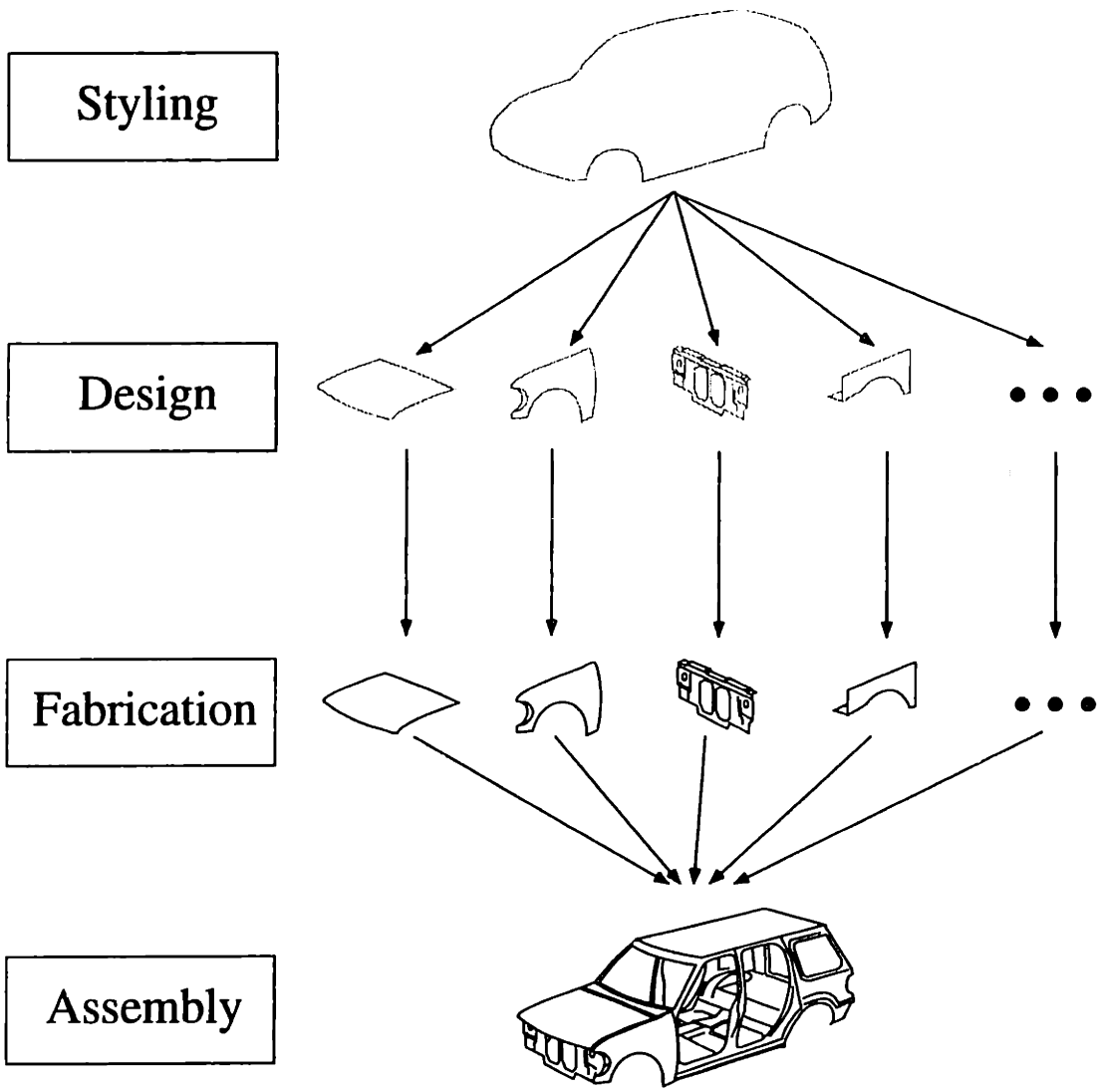

Figure 1.1 Flow of the automobile body development process

Typical causes of variation-related assembly problems are identified using a cause-and-effect analysis, e.g., Ishikawa fishbone diagram. Figure 1.2 shows the results of such an analysis. Broadly speaking, there are three major sources of assembly problems.

- Parts are designed incorrectly
- Parts are manufactured incorrectly
- Parts are assembled incorrectly

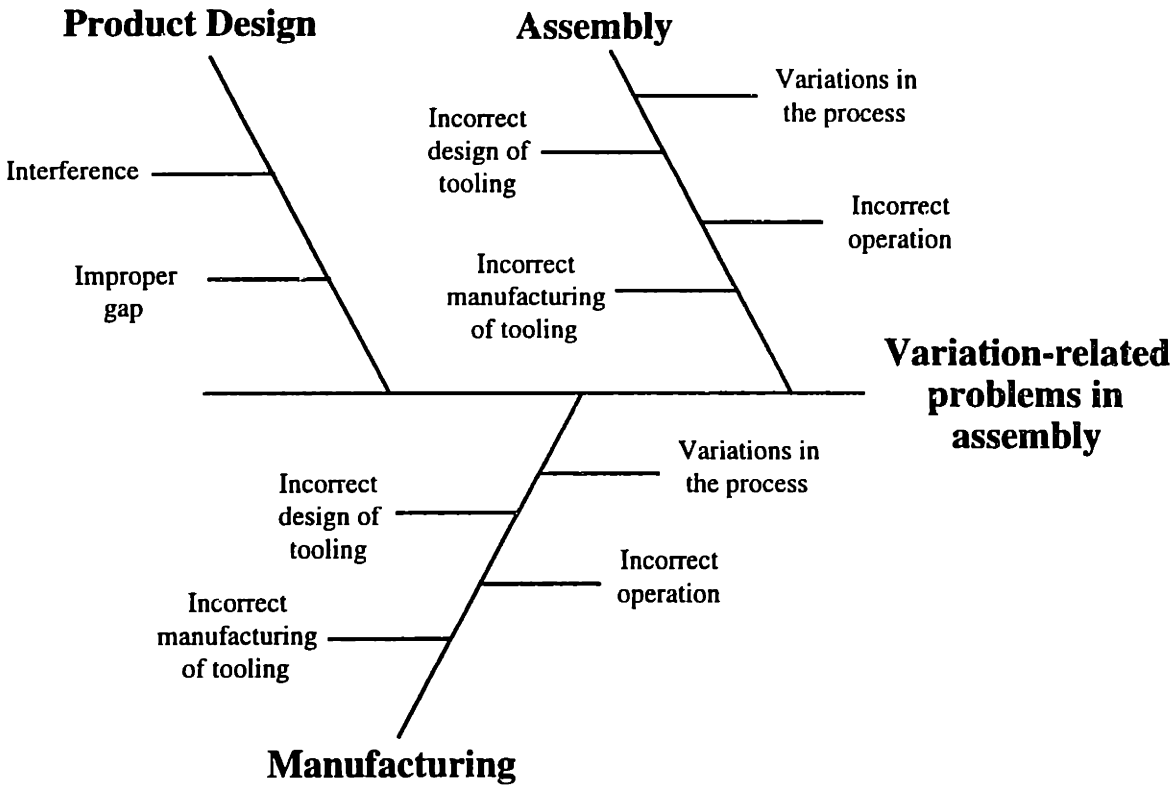

Figure 1.2. Sources of variation-related assembly problems

1.2.1. Parts are designed incorrectly

Very often, variations are caused by incorrect design of parts; if component parts are designed incorrectly, then the assembly will have problems even if parts are perfectly manufactured. For example, if contours of the door and the door aperture are designed such that they do not match, i.e., interfere with each other or have a too-large gap, then variations will arise in the assembly, even if the parts are manufactured perfectly.

1.2.2. Parts are manufactured incorrectly

Even though parts are designed perfectly, they cannot be manufactured perfectly because of inherent variations in the manufacturing process. In addition to inherent variations in the manufacturing process, sometimes manufacturing process is designed, implemented, or maintained incorrectly due to human errors so that manufactured parts do not match the

design. For example, the die surface is designed incorrectly or the stamping process parameters, e.g., press tonnage or line speed, are set incorrectly.

1.2.3. Parts are assembled incorrectly

Even though parts are perfectly designed and manufactured, they cannot be assembled perfectly because of inherent variations in the assembly process. Also sometimes the assembly process is designed, implemented, or maintained incorrectly so that parts are distorted during the assembly process and remain deformed in the assembly. For example, if fixtures locate parts in the wrong position, then welding guns weld parts incorrectly.

1.3. Problem statements and goals

Since most current computer-aided design (CAD) systems today are based on ideally-sized and ideally-located rigid geometry, they are unable to model, or predict, the effects of variations in parts and tooling in assemblies consisting of compliant parts. Within this context, a framework for the consideration of part deformation and variations in parts and tooling is required in order to obtain more effective CAD systems.

The goal of this thesis is to provide a conceptual framework for modeling the assembly of compliant parts with dimensional variations to predict propagation of variations in assembly. The following are the potential benefits of this research.

- Identify dimensions in parts and tooling that contribute to variations in critical dimensions of the final assembly so that such dimensions can be carefully designed, produced, and monitored.

- Anticipate potential assembly problems before expensive parts and tooling are produced so that these problems can be avoided early in the product development cycle when the time and cost required for engineering change is relatively small.

- Trace existing assembly problems back to their root cause(s) effectively after problem is encountered. Practically speaking, not all assembly problems can be anticipated and avoided before they happen. When problems happen on the production floor, time is very critical. An assembly model that links causes and symptoms will make diagnosis easier, faster, and more effective.

- Evaluate how the design of product, tooling, and assembly process is robust to variations in incoming parts. Depending on the design, the way variations in incoming parts propagate changes. One of the criteria for good design is how the design is robust, or insensitive, to variations in incoming parts. This research will provide a rationale for comparing design alternatives.

1.4. Overview of thesis

This thesis proposes an integrated framework that gives CAD systems the capability to model the effects of variations in compliant parts and tooling. The approach consists of (1) mathematical methods to represent assembly of compliant, non-ideal parts in CAD systems and (2) procedures to simulate propagation of variations in assembly.

Chapter 2 reviews existing work that is closely related to this thesis.

Chapter 3 identifies the basic concepts to be represented for examining the effects of variations in parts and tooling: component parts, assembly tooling, features, interaction between mating features, variations in parts and tooling, and deformation of parts and its relationship to various forces during assembly. A mathematical approach is developed to represent these concepts in future CAD systems.

Chapter 4 uses these methods to model assembly of compliant, non-ideal parts and simulate propagation of variations. Two new concepts are presented: *PCFR cycle* and *contact chain*. Complex assembly processes are modeled as a series of PCFR cycles, each

of which consists of four steps: place, clamp, fasten, and release. The relationship between parts and tooling in the PCFR cycle is represented by contact chains, i.e., closed loops of mating features. Simulation procedures are presented to predict the effects of variations in parts and tooling in assembly.

Most of the work presented in Chapter 3 and 4 has been implemented and tested with an experimental software package. Chapter 5 presents the results of simulations for several assemblies.

Chapter 6 presents some of the applications implemented based on the proposed assembly model. First, dimensions that contribute to critical dimensions of an automobile front-end assembly are identified from sensitivity analysis. Second, robustness of design alternatives is evaluated based on the sensitivity analysis. Third, computational methods for diagnosing assembly problems are presented with a case study.

2

Related Work

Previous work that is closely related to this thesis is roughly divided into three areas: modeling variations in parts, modeling the assembly of non-ideal parts, and applying assembly models at various stages of the product development process: design, pre-production, and production.

2.1. Interpretation of variations in parts

Tolerances define acceptable variations in geometry. There are currently two major approaches on physical interpretation of tolerances in parts: parameter space and true positioning approach. This section briefly describes these approaches[1].

2.1.1. Parameter space approach

Objects are defined by a set of parameters such as the distance and angle between geometric entities, e.g., vertex or line. Dimension is considered to define the relationship between two geometric entities, and tolerance is considered to be an acceptable variation in that relationship. Authors who have made extensive use of the parameter space approach

[1] More detailed discussion can be found in the survey papers by Gossard [Gossard 88], Juster [Juster 92], and Roy [Roy 91].

include Hillyard [Hillyard 78], Hoffman [Hoffman 82], Light [Light 82], and Turner [Turner 87].

2.1.2. True positioning approach

Each geometric entity is considered to possess some absolute position in space. Tolerances are then zones of space that define regions in which the geometric entity must exist. The current A.N.S.I. standard on dimensioning and tolerancing [ANSI Y14.-1995] defines true positioning. Researchers who have adopted this approach include Requicha [Requicha 83] and Srinivasan [Srinivasan 89].

2.1.3. Discussion

The parameter space approach provides a better computational framework for many existing applications such as tolerance analysis and synthesis. On the other hand, the true positioning approach can represent more diverse types of tolerances, e.g., straightness, roundness, cylindricity, or profile. Unfortunately, these approaches are not interchangeable as mentioned by Requicha [Requicha 83]. Currently, both approaches are used in academia and industry.

2.2. Assembly modeling

The assembly process is often considered as a process of determining the relative position of parts in an assembly. Part position is often represented by a homogeneous transformation matrix[2]. Relative position of parts is found from spatial relations between mating features, e.g., the centerlines of a pin and a hole are aligned (fit), the normal vectors of two planar surfaces are opposite to each other (against).

[2]See Appendix A

2.2.1. Assembly model of ideal parts

When parts are ideal, such spatial relations can be represented as equality constraint equations. Because these equations are non-linear in three dimensional space, these equations are solved by Newton-Raphson method or least square method. When dimensions of individual parts change, their relative positions can be updated by solving the set of constraint equations. Solutions to this problem are provided by Ambler [Ambler 75] and Lee [Lee 85, Rocheleau 87].

2.2.2. Assembly model of non-ideal parts

When parts are not ideal, the spatial relations such as fit and against are not always satisfied. Consider a pin and an oversized hole. The centerlines of a pin and hole are not necessarily aligned in assembly. Three approaches trying to overcome such a limitation have been reviewed.

Range of part positions

Fleming [Fleming 88] developed a method to find the range of part positions in an assembly for given ranges of part errors. In his approach, spatial relations are modeled as inequality constraint equations from non-interference requirements. Then, the possible range of part positions are calculated from the inequality constraint equations.

Optimal part positioning

Turner [Turner 87] formulated part positioning into a constrained optimization problem. In his formulation, the variables are part positions, the constraints are non-interference requirements, and the objective function is the sum of the gap between each mating pair. He claimed that parts are positioned in an assembly such that the objective function is minimized.

Contact states search

Inui and Kimura [Inui 91] proposed an alternative approach to find the most likely positions of parts in an assembly. They claimed that a mating pair ends up in three possible contact states: single vertex contact, two vertices contact, or three or more vertices contact. Their approach is to search all possible part positions in an assembly (assuming that mating features are always in contact), and select the configuration that maximizes the number of contact points between parts. The underlying assumptions are that (1) parts settle in the most stable configuration, and (2) parts are most stable in an assembly when the number of contact points is maximized.

2.2.3. Discussion

There are two major limitations in the above assembly models.

- In the presence of forces, parts deform during assembly and remain deformed after assembly. Sometimes, errors due to part deformation is larger than manufacturing errors in incoming parts and therefore cannot be neglected. Part deformation in assembly and its effects on variations in the assembly have not been covered by previous work.

- Variations in an assembly are affected by the assembly tooling as well as component parts. The effects of variations in assembly tooling are not considered in most literature.

2.3. Tolerance analysis and synthesis

Currently, tolerance analysis and synthesis are the most common applications where assembly models of non-ideal parts are used. Tolerance analysis predicts how variations in parts sum in an assembly, while tolerance synthesis economically allocates tolerances to

parts still meeting the tolerance specification in an assembly. This section briefly describes literature on tolerance analysis[3].

2.3.1. Worst case versus root sum square

The two most common models for tolerances are the worst case model and the root sum square model. Let the assembly dimension of interest be y

$$y = f(x_1, x_2, \cdots, x_N) \qquad \text{Eq. 2.1}$$

where x_i's are the dimensions and N is the number of component dimensions that affect y. Worst case and root sum square models fot the variations in y are shown in Eq. 2.2 and 2.3.

Worst Case Model

$$\Delta y = \sum_i^N \left(\frac{\partial y}{\partial x_i} \Delta x_i \right) \qquad \text{Eq. 2.2}$$

where Δy is the variation in y and Δx_i is the variation in x_i.

Root Sum Square Model

$$\sigma_y = \sqrt{\sum_i^N \left(\frac{\partial y}{\partial x_i} \sigma_i \right)^2} \qquad \text{Eq. 2.3}$$

where σ_y is the standard deviation of y and σ_i is the standard deviation of x_i.

Worst case model assumes that all part dimensions occur at their worst limit simultaneously. It is used to assure that all assemblies meet the specified limit. On the other hand, root sum square model assumes that component variations have a normal (or

[3] More detailed discussion can be found in the survey papers by Roy [Roy 91], Chase [Chase 91], and Turner [Turner 95].

Gaussian) distribution with a zero mean. Root sum square model is used to predict distribution of assembly variations[4].

Fortini [Fortini 67] and Bjorke [Bjorke 89] provide extensive discussion of tolerance analysis. Later Turner [Turner 87] and Fleming [Fleming 88] automated tolerance analysis based on their assembly models. There also exist commercial software for automated tolerance analysis [VSA 95].

2.3.2. Discussion

Good tolerance analysis depends on (1) accurate estimation of component variations, (2) accurate assembly models to predict propagation of variations in assembly, and (3) statistical techniques for adding two or more variables with certain distributions. Currently, most literature emphasizes the third.

2.4. Diagnosis of variation-related assembly problems

A relatively less explored application where assembly models are used is the diagnosis of assembly problems, i.e., identifying the cause(s) of existing abnormal assembly variations. While tolerance analysis and synthesis are useful concepts for design, computational tool for diagnosis is beneficial during pre-production and production.

A diagnostic problem is a problem in which one is given a set of symptoms and must explain why they are present by using one's knowledge about the system. Symptoms are very different depending on the nature of problem domain; sometimes they are discrete, continuous, or even non-parametric. Diagnostic mechanisms differ from each other significantly for different problem domains.

---

[4]There exist other more sophisticated statistical methods to predict distribution of assembly variations, e.g., estimated mean shift model, Monte Carlo simulation, etc. For more details, refer to the papers by Chase [Chase 91] and Turner [Turner 95].

2.4.1. Diagnosis of automobile body assembly

Very little literature exists for diagnosis of variations in mechanical assemblies [Hu 92, Ceglarek 94]. Hu and Ceglarek divide the diagnosis process into two steps: (1) fault symptom detection and (2) root cause detection. In the first step, correlation of measurement data is studied using Principal Component Analysis, which helps to understand patterns of variations. In the next step, the patterns are compared with the table shown in Table 2.1.

Root causes		Fault symptoms	
Identification	Description	Direction of deformation	Area of deformation
locators pins	mislocated, worn out, loose, missing	perpendicular to the centerline of pins	global
clamps	not functioning, missing, not closing properly	normal to the clamping surface	global
welding guns	unequalized welding gun, worn out tip, missing welding spot, malfunction of tip dressing operation	normal to the direction welding guns approach	local
External interference		any direction	local

Table 2.1 Root cause - symptom relation table provided by Ceglarek et al.[Ceglarek 94]

(Unfamiliar terminologies are substituted by more general terms)

2.4.2. Discussion

The diagnostic mechanism in the domain of variations in mechanical assembly is based on experience rather than a concrete computational basis. Actual relations between causes and symptoms are much more complex than those listed in Table 2.1. Furthermore, assembly problems are often due to multiple causes. When multiple causes occur simultaneously, the use of look-up tables is likely to fail.

3

Representation

In order to model assemblies of compliant, non-ideal parts, the following concepts need to be represented.

- Components
- Mating features
- Dimensional errors, i.e., variations
- Force, displacement, and constitutive relations

This chapter describes methods to represent the above concepts.

3.1. Nomenclature

In describing the above concepts, the folowing notations will be used.

Objects and Features

- parts: A (italic upper case)
- tooling & fixtures: $\underline{A}$ (italic with underbar)

- features: $A.i$ (italic upper case . number)

Coordinate Frames

- $\mathcal{Ref}$: reference coordinate frame
- $\mathcal{A}$: body coordinate frame of A
- $\mathcal{A}.i$: feature coordinate frame of $A.i$

Displacement vectors

displacement vector: $\mathbf{v} = \{x \quad y \quad z \quad \psi \quad \theta \quad \phi\}^T$

where x, y, and z correspond to translational displacements, while ψ, θ and ϕ correspond to rotational displacements.

vector $\mathbf{v}$ with respect to a coordinate frame $\mathcal{R}$: ${}^{\mathcal{R}}\mathbf{v}$

elements of $\mathbf{v}_{A.i}$: $v_{A.i,x}$, $v_{A.i,y}$, ...

- ${}^{\mathcal{B}.j}\lambda_{A.i}$: relative position of $A.i$ with respect to $\mathcal{B}.j$
- $\delta_{A.i}$: displacement of $A.i$ due to manufacturing imperfections
- $\upsilon_{A.i}$: displacement of $A.i$ during assembly
- $\varepsilon_{A.i}$: total displacement of $A.i$
- $\mathbf{f}_{A.i}$: force/moment applied to $A.i$

3.2. Components

3.2.1. Geometry

An automobile body consists primarily of sheet metal panels. Sheet metal panels can be represented by surfaces in a parametric form,

$$\mathbf{r} = \mathbf{r}(u, v), \qquad \text{Eq. 3.1}$$

where u and v are parametric variables, and $\mathbf{r}$ is a vector function that maps a point in two dimensional parametric space spanned by u and v to a point in three dimensional object space as shown in Figure 3.1.

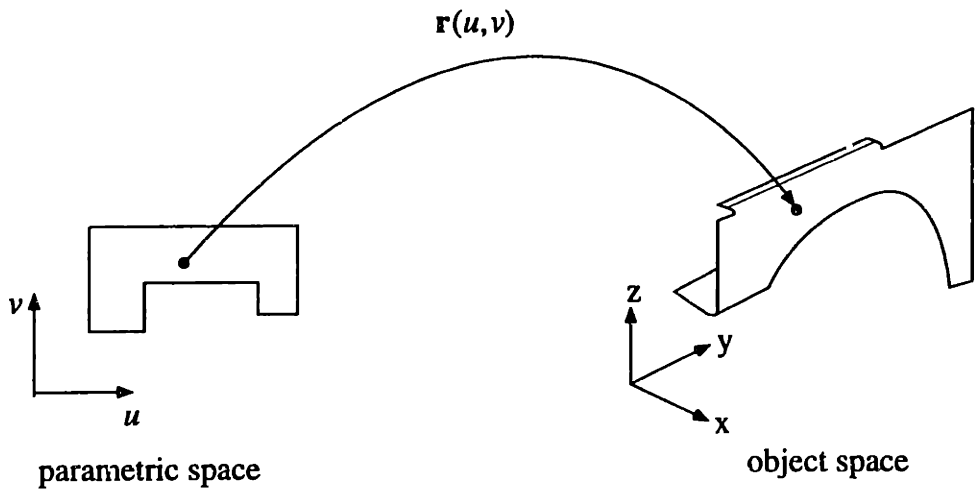

Figure 3.1 Parametric representation of a surface

3.2.2. Features

For the purpose of this thesis, features are defined as geometric entities on parts that are important for functionality, manufacturing, assembly, appearance, etc. Examples include locator pins, holes, and clamping surfaces.

The position of a feature can be represented using an imaginary coordinate frame attached to the feature, i.e., feature coordinate frame, as shown in Figure 3.2. The position of a coordinate frame is represented by the homogeneous transformation matrix[1]:

$$\mathbf{T} = \left[\begin{array}{c|c} \mathbf{R} & \mathbf{t} \\ \hline 0\ 0\ 0 & 1 \end{array}\right] \qquad \text{Eq. 3.2}$$

where $\mathbf{R}$ is the 3×3 transformation matrix that defines the rotation of the coordinate frame, and $\mathbf{t}$ is the 3×1 vector that defines the translation of the coordinate frame with respect to the reference frame.

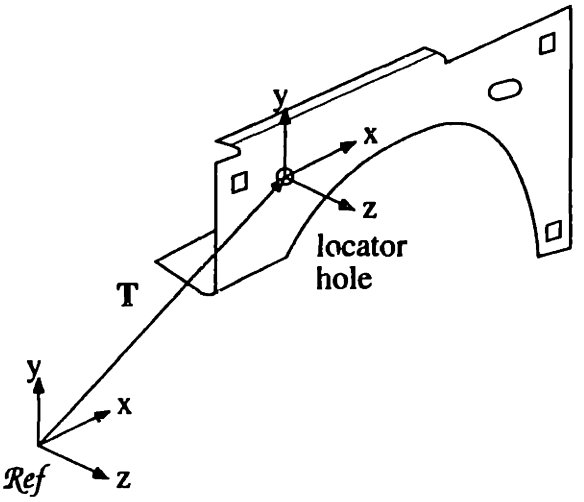

Figure 3.2 Position of a feature

3.2.3. Graph representation

A part can then be considered as a graph of features as shown in Figure 3.3. Features are connected to each other by the material between the features, e.g., sheet metal for automobile body panels. If the material between the features is rigid, then the relative positions of features are fixed. Otherwise, their relative positions are constrained by the compliance of the material between the features.

[1]See Appendix A

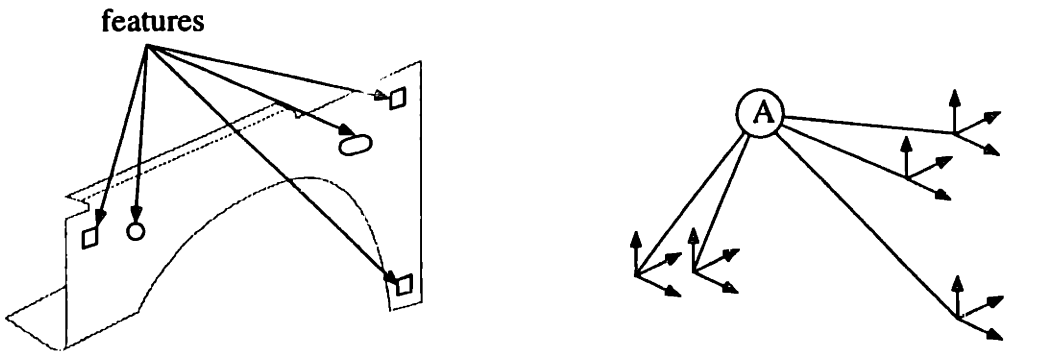

(a) Part A (b) Graph representation of part A

Figure 3.3 Graph representation of a part

3.3. Mating features

During assembly, parts come into contact with other parts and assembly tooling. Features on parts or tooling that contact other objects during assembly are called mating features. Broadly, mates between features are categorized into two types:

- 0-dof[2] mate: 0-dof mates are mates where relative motions between the mating features are not allowed. 0-dof mates are made by welding, bolting, gluing, etc. In automobile body assembly, 0-dof mates usually exist between parts.

- n-dof mate: n-dof mates are mates where features can move relative to each other. Examples include pin/hole, edge/plane, plane/plane mates. In automobile body assembly, n-dof mates usually exist between parts and tooling.

Relative motion between mating features can be decomposed into a translation and a rotation. Translation is described by a translation vector,

[2]degrees of freedom

$$\lambda_t = \begin{Bmatrix} \lambda_x \\ \lambda_y \\ \lambda_z \end{Bmatrix}. \qquad \text{Eq. 3.3}$$

Rotation can be described by the axis of rotation and the magnitude of rotation, and is represented by a rotation vector,

$$\lambda_r = \begin{Bmatrix} \lambda_\psi \\ \lambda_\theta \\ \lambda_\phi \end{Bmatrix} \qquad \text{Eq. 3.4}$$

where the magnitude of λ_r, i.e., $|\lambda_r|$, is the magnitude of rotation, and the direction of λ_r is the axis of rotation; direction cosines of the axis of rotation are

$$\frac{\lambda_\psi}{|\lambda_r|}, \ \frac{\lambda_\theta}{|\lambda_r|}, \text{ and } \frac{\lambda_\phi}{|\lambda_r|}. \qquad \text{Eq. 3.5}$$

in the x, y, and z directions, respectively. Translation and rotation of a feature are collectively represented by a 6×1 vector:

$$\lambda = \begin{Bmatrix} \lambda_x \\ \lambda_y \\ \lambda_z \\ \lambda_\psi \\ \lambda_\theta \\ \lambda_\phi \end{Bmatrix}. \qquad \text{Eq. 3.6}$$

In an n-dof mate, relative motion between mating features is constrained by the shape of the mating features. For example, if mating features are cylindrical, as in the case of a pin and hole mate, then the features can translate and rotate around the common centerline, but other motions are restricted. Allowable relative motion between features can be represented by constraints imposed on the elements of λ. For example, the allowable

relative motion between the pin and hole in Figure 3.4 having the same diameters and whose centerlines lie on the z-axis can be represented as

$$\lambda = \begin{Bmatrix} 0 \\ 0 \\ \lambda_z \\ 0 \\ 0 \\ \lambda_\phi \end{Bmatrix} \qquad \text{Eq. 3.7}$$

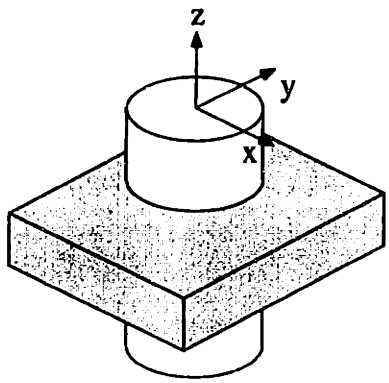

Figure 3.4 Pin/hole mate

In most mating features in an automobile body assembly[3], there exist coordinate frames in which constraints imposed on relative motion can be represented by simply assigning zero values to the element(s) of λ as in Eq. 3.7. As coordinate frames of features can be chosen arbitrarily, a coordinate frame in which constraints imposed on relative motion can be represented easily is chosen as the feature coordinate frame[4].

3.4. Variations

The variation of a feature is the difference in shape and position between the actual feature and the ideal feature specified by the design. Broadly speaking, variations can be classified into two categories: shape errors and position errors.

---

[3]Exceptions include screw bolts and nuts, gears, cams and followers.
[4]Motions described by 6x1 vectors in a feature coordinate frame can be described in any other coordinate frame (See Appendix B).

A shape error refers to a deviation of a feature from its nominal shape, e.g., circularity of a hole, diameter of a hole, and flatness of a planar surface. On the other hand, a position error refers to a displacement of a feature from its nominal location and orientation, e.g., location of a hole and orientation of a planar surface. Figure 3.5 illustrates shape error and position error of a hole and a planar surface. Because shape errors in mating features are very small compared to position errors in automobile body assembly[5], this thesis deals only with position errors.

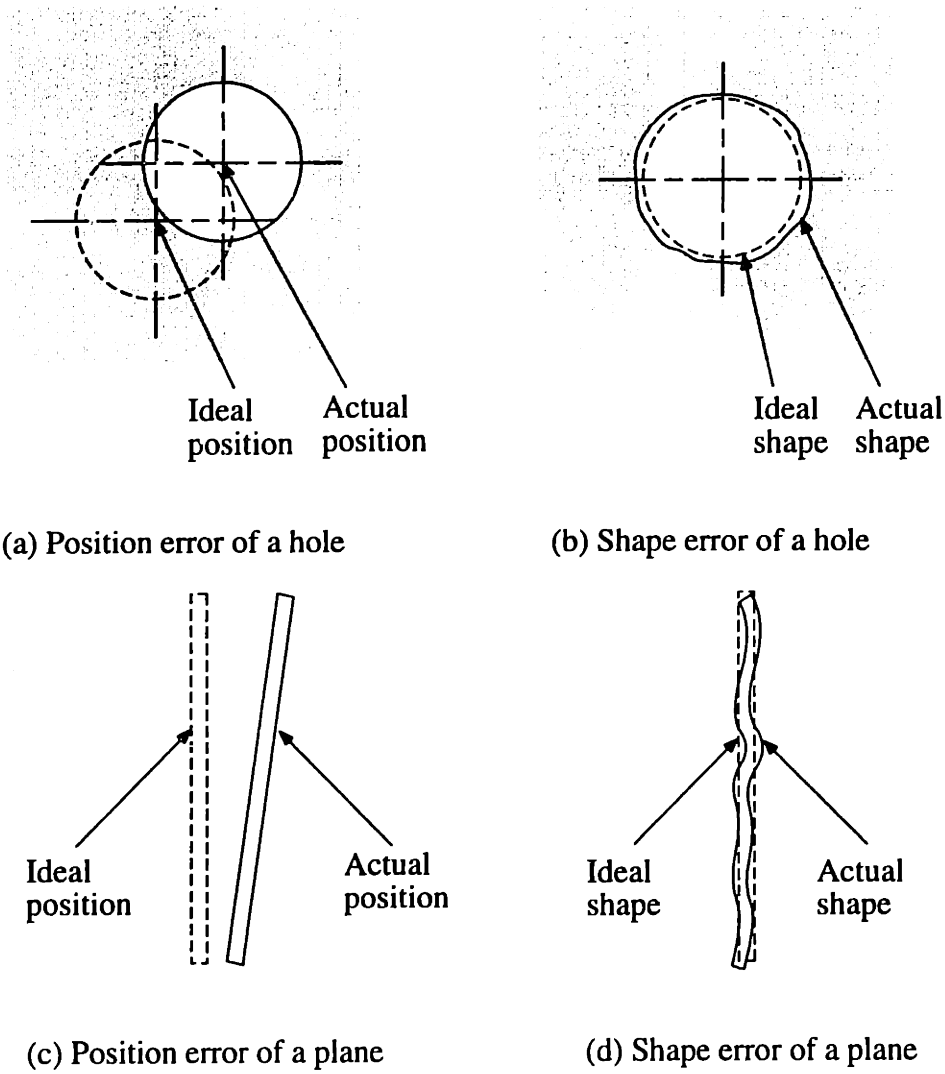

(a) Position error of a hole

(b) Shape error of a hole

(c) Position error of a plane

(d) Shape error of a plane

Figure 3.5 Shape errors and position error

[5]See Appendix C

In order to discuss position errors of a feature, the object that contains the feature must be positioned with respect to the reference frame. A set of locators that uniquely, but not redundantly, define a part's position is called *a complete locator scheme.* A complete locator scheme is designated to every part and assembly. An illustration of a complete locator scheme is presented in Figure 3.6.

- Three primary points restrict translation along the z-axis and rotations about the x and y-axes.
- Two secondary points restrict translation along the x-axis and rotation around the z-axis
- A tertiary point restricts translation along the y-axis.

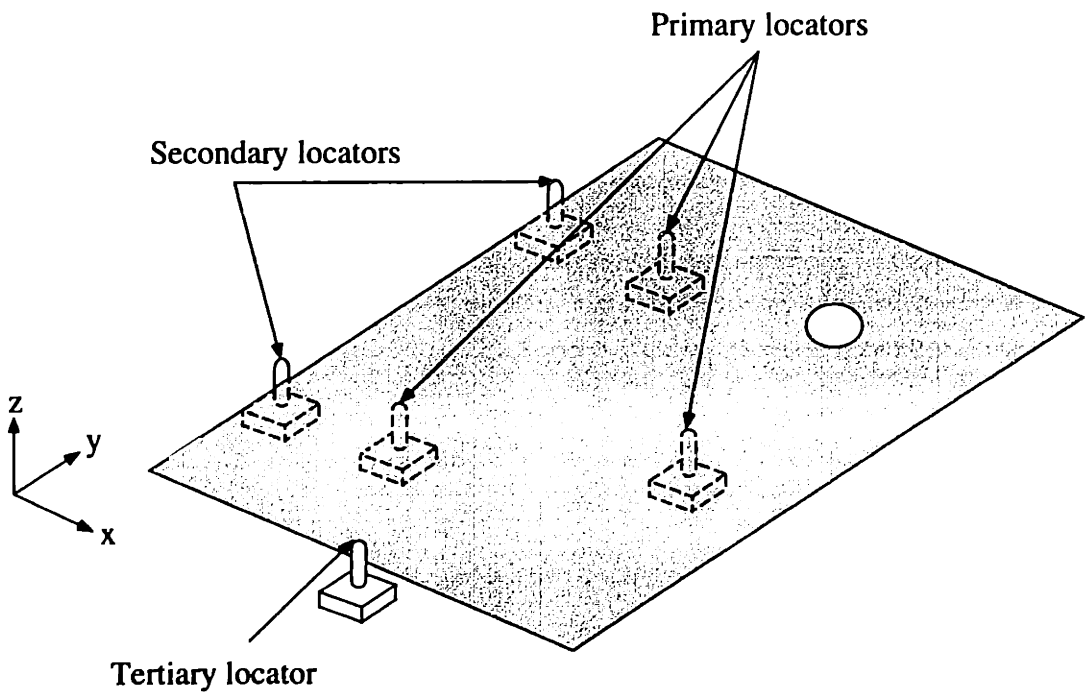

Figure 3.6. 3-2-1 locator scheme

Let $\tilde{A}$ be a manufactured instance of part A. Suppose that $\tilde{A}$ is positioned by its designated complete locator scheme as shown in Figure 3.7. Then, the position error of a

feature δ is the discrepancy between the ideal and the actual position of the feature coordinate frame.

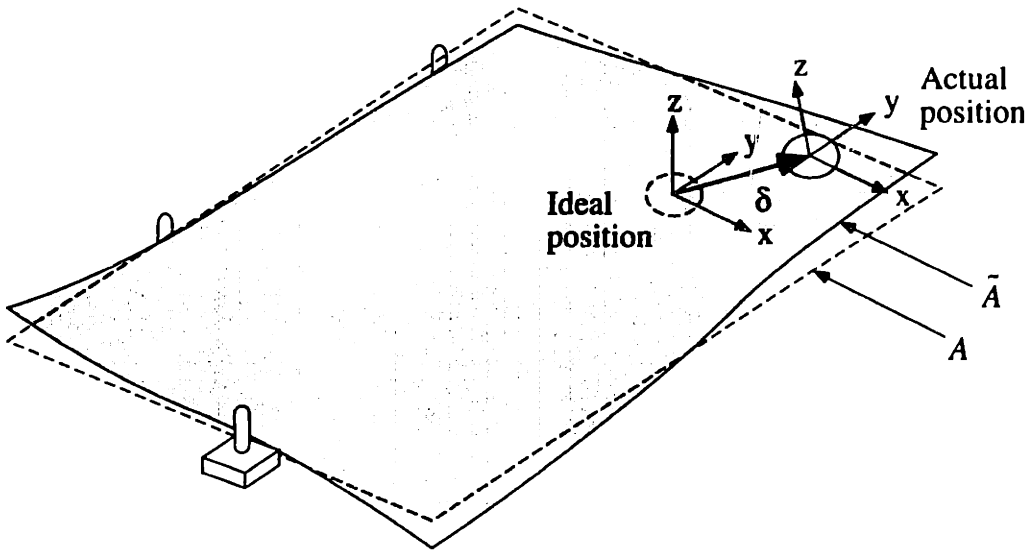

Figure 3.7 Position error of a feature

Position error of a feature can be represented by a 6×1 vector similar to the representation used for relative motion:

$$\delta = \begin{Bmatrix} \delta_x \\ \delta_y \\ \delta_z \\ \delta_\psi \\ \delta_\theta \\ \delta_\phi \end{Bmatrix}. \qquad \text{Eq. 3.8}$$

where δ_x, δ_y, and δ_z correspond to translation, and δ_ψ, δ_θ, and δ_ϕ correspond to rotation with respect to the ideal feature coordinate frame.

Position errors in certain directions are neither defined, nor can they be measured depending on the shape of features. For example, the rotation error of a hole about its centerline cannot be defined due to symmetry. Such position errors that cannot be defined

are assumed to be zero. For example, the position error of a hole whose centerline lies is along the z-axis is

$$\delta = \begin{Bmatrix} \delta_x \\ \delta_y \\ \delta_z \\ \delta_\psi \\ \delta_\theta \\ 0 \end{Bmatrix}. \qquad \text{Eq. 3.9}$$

3.5. Force, displacement, and constitutive relations

During the assembly process or in the final assembly, parts deform from their nominal shapes and move from their ideal positions. As a result, feature positions change. Displacement of a feature is represented by a 6×1 vector similar to the manner in which relative motion and position error are represented:

$$\upsilon = \begin{Bmatrix} \upsilon_x \\ \upsilon_y \\ \upsilon_z \\ \upsilon_\psi \\ \upsilon_\theta \\ \upsilon_\phi \end{Bmatrix}, \qquad \text{Eq. 3.10}$$

where υ_x, υ_y, and υ_z correspond to translation, and υ_ψ, υ_θ, and υ_ϕ correspond to rotation with respect to the ideal feature coordinate frame.

Displacement of features are coupled by constitutive relations. For parts with simple geometries, constitutive relations can be calculated by solving the differential equations of equilibrium. When part geometry can be approximated as an assembly of simple structural elements, such as beams and trusses, constitutive relations can be obtained by applying matrix operations to the constitutive relations of simple structural elements [Martin 66, Kardestuncer 74]. When part geometry is complex, constitutive relations can be obtained

from the mathematical representation of part geometry as in Eq. 3.1 using finite element methods[6] [Bathe 82, Reddy 93].

If deformations are small and material properties are linear, constitutive relations can be represented in the form,

$$\mathbf{f} = \mathbf{K}\mathbf{u}, \qquad \text{Eq. 3.11}$$

where $\mathbf{f}$ is a vector representing external forces acting on the nodes, $\mathbf{u}$ is a vector representing displacements of the nodes, and $\mathbf{K}$ is the corresponding stiffness matrix.

If we assume that forces are applied only on mating features, Eq. 3.11 can be condensed to the form[7],

$$\mathbf{f}_m = \mathbf{K}_m \mathbf{u}_m, \qquad \text{Eq. 3.12}$$

where $\mathbf{u}_m$ is the displacement vector of the mating features,

$$\mathbf{u}_m = \begin{Bmatrix} \underline{\upsilon_1} \\ \underline{\upsilon_2} \\ \underline{\vdots} \\ \underline{\upsilon_i} \\ \underline{\vdots} \\ \underline{\upsilon_N} \end{Bmatrix} \text{ (υ_i is the displacement of the i-th mating feature),} \qquad \text{Eq. 3.13}$$

$\mathbf{f}_m$ is the force vector acting on the mating features and $\mathbf{K}_m$ is the corresponding stiffness matrix.

3.6. Summary

Key points described in this chapter can be summarized as,

---

[6]There exist methods to obtain constitutive relations automatically from mathematical representation of part geometry [Shimada 93].
[7]See Appendix D

- Parts are modeled as a graph of features that are represented by coordinate frames.

- Relative motion between mating features is constrained by the shape of the mating features, and is represented by a vector λ. Spatial relations of mating pairs are represented by constraints on the elements of λ.

- Position error of features is modeled as the displacement of feature coordinate frames, and is represented by a vector δ.

- Displacement of features during the assembly process and in the resultant assembly is represented by a vector υ, which is constrained by constitutive relations.

4

Assembly Modeling

This chapter presents a new assembly model for predicting variations in the assembly of compliant, non-ideal parts. For given variations in parts and assembly tooling, the proposed method simulates propagation of the variations as parts go through the assembly process.

The first two sections describe the representation method for assembly processes and interactions between parts and assembly tooling during the assembly process.

Section 4.3, 4.4, 4.5 and 4.6 explain procedures to simulate the assembly process.

Section 4.7 reviews the key points discussed in this chapter.

4.1. Unit of assembly process: PCFR cycle

An automobile body is assembled through hundreds of assembly stations; parts are assembled into a subassembly at one station, the subassembly is transferred to the next station to be assembled into a bigger subassembly, and so on. This process continues until the final product is assembled. Figure 4.1 illustrates a small portion of the lengthy process of automobile body assembly. Variations in incoming parts and in assembly tooling

propagate through this process and cause variations in the final assembly such as uneven margins between the hood and fenders.

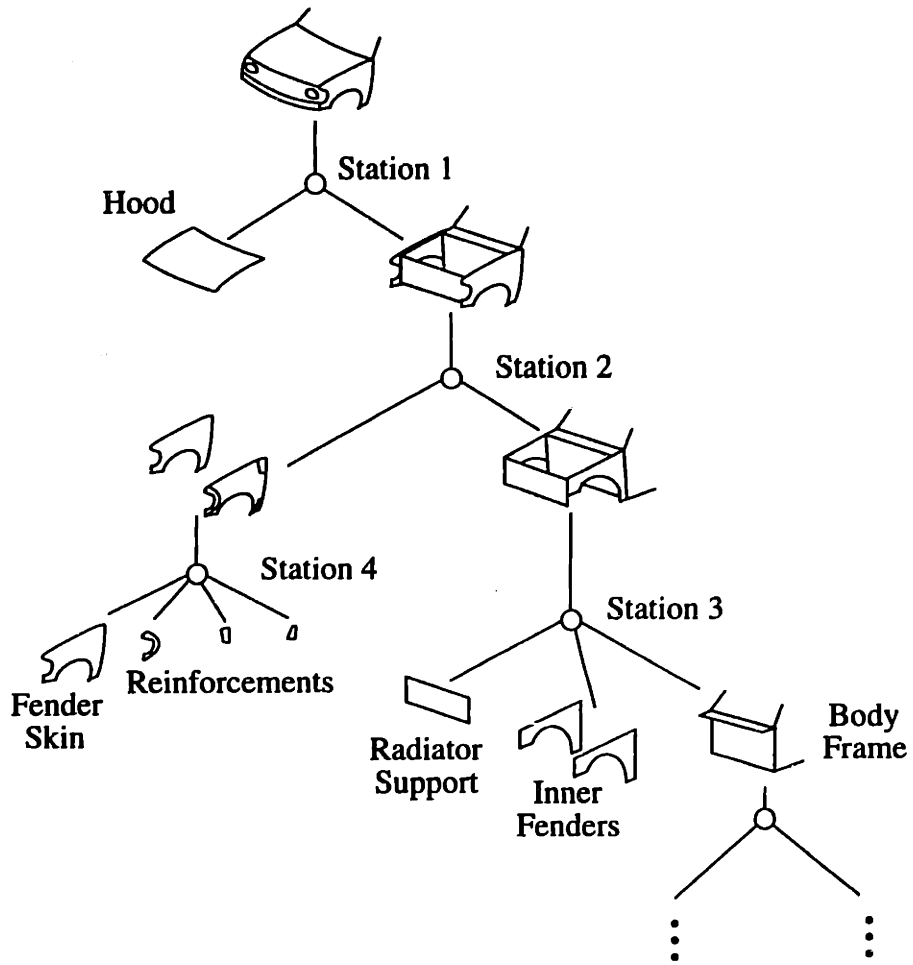

Figure 4.1 Assembly process of automobile body

At each assembly station, parts (or subassemblies) are assembled through a cycle that consists of four steps: Place, Clamp, Fasten and Release. This cycle is an elementary structure of a complex assembly process, and is called a *PCFR cycle*. Figure 4.2 illustrates a PCFR cycle for the assembly of two C-shaped parts. In this figure, (a), (c), (e), and (g) illustrate the ideal PCFR cycle, while (b), (d), (f), and (h) illustrate an actual PCFR cycle when parts and assembly tooling are not ideal.

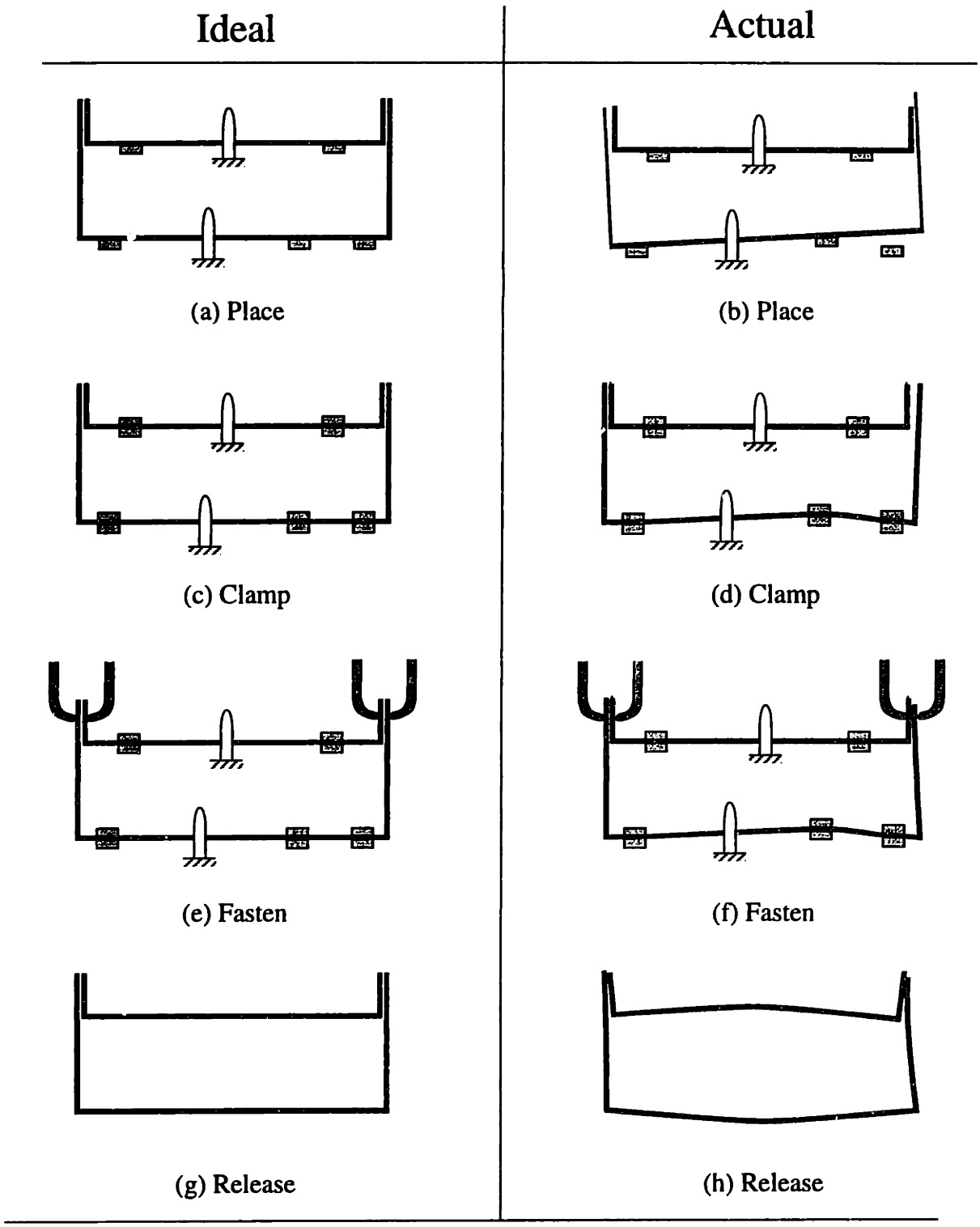

Figure 4.2. PCFR cycles

Place

Parts are first placed in an assembly fixture as illustrated in Figure 4.2 (a). The location and orientation of parts are determined by mating features between the parts and the assembly fixture. Typical mating features for placing parts are pin/hole, pin/slot, block/surface, and block/edge mating features. These features are often called locator features.

In the actual process, parts move from their nominal positions as illustrated in Figure 4.2 (b) because of variations in the mating features of the parts and assembly tooling.

Clamp

Once parts are placed, they are clamped as illustrated in Figure 4.2 (c). Clamps prevent parts from being detached from locator blocks during assembly. Ideally, clamps should barely touch the parts; however, in the actual process, clamps often deform parts as illustrated in Figure 4.2 (d) because parts or clamps are not in the ideal position.

Fasten

Once parts are clamped, they are fastened. The most commonly used fastening process for automobile body assembly is spot welding. Spot welding is done mostly by automatic welding guns. A welding gun is connected either to an assembly fixture or to a robot. Each welding gun is programmed to move to a certain position and grasp the parts to be welded with its fingers. An electric current is then passed through the parts in a concentrated area to form a metal nugget between the welding surfaces.

Welding guns are similar to clamps in that the welding guns pull or push parts during grasping when the welding surfaces or welding guns are not in their ideal positions as illustrated in Figure 4.2 (f). It is important that when welding surfaces or welding guns are not in their ideal positions, the locations of actual welding points are different from their

ideal locations. This welding spot change is one of the major causes of assembly variations.

Release

Once parts are fastened, they are finally released from the fixture. Because of the various errors explained above, parts are often deformed in the fixture. When parts are released from the fixture, they spring back to minimize the total strain energy stored in the assembly. Very often, parts remain deformed in the assembly as illustrated in Figure 4.2 (h) even after the assembly has been released from the fixture.

4.2. Graph representation of the PCFR cycle: Contact chain

As described in the previous section, assembly is done in a sequential manner; the product is assembled through a series of assembly stations, and also at each station, parts (or subassemblies) are assembled in the following sequence: place, clamp, fasten, and release. The fact that parts are assembled in a sequential manner is often neglected in previous work[1].

Another very important point overlooked in previous work is the role of assembly tooling during the PCFR cycle; parts are placed and clamped by fixtures and welded by welding guns. At each step new contacts are established until the fastening step, after which the contacts between the parts and assembly tooling are broken during the release step. The only mates that remain after the release step are the weld joints between parts; the position of which are determined by the history of the place, clamp, and fasten process. In order to model the effects of variations in parts and assembly tooling, (1) the interaction between parts and tooling and (2) its change over the PCFR cycle need to be modeled.

[1] See section 2.2

The interaction between parts and tooling at each step of the PCFR cycle can be represented by a graph of mating features called the *contact chain*. Figure 4.3 (b) illustrates the contact chain of parts and assembly tooling during the fasten step shown in Figure 4.3 (a). Each oval node depicts a part or assembly tooling. Each solid node depicts a contact between mating features where force interactions take place. Each edge depicts a connection between features on parts.

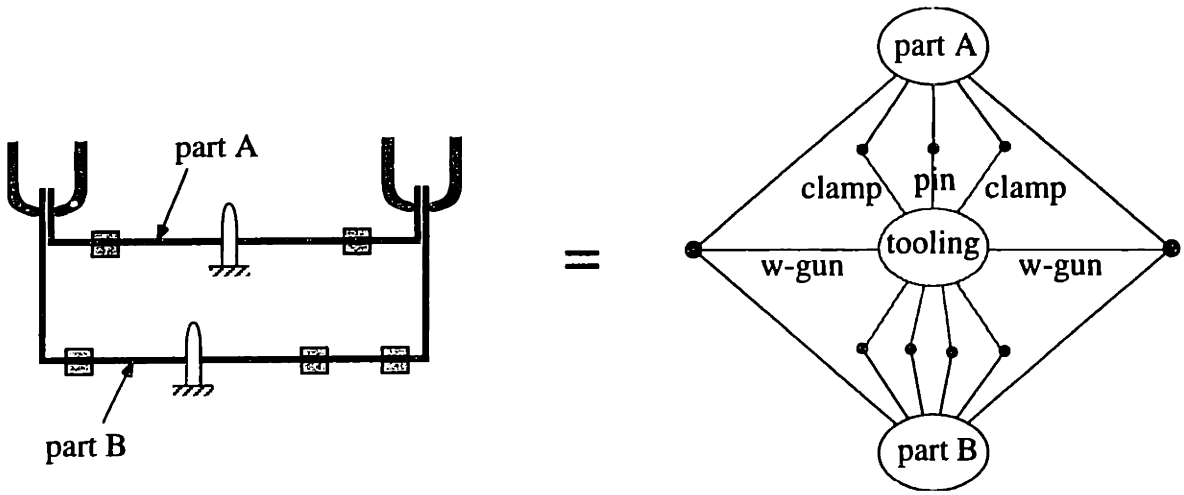

(a) Physical parts and tooling (b) Contact chain

Figure 4.3 Graph representation of interaction between parts and tooling

Likewise, the interaction between parts and tooling at each step of the PCFR cycle can be represented as shown in Figure 4.4.

At every step of the PCFR cycle, each object must satisfy the constitutive relation. At each contact node, geometric compatibility and force continuity must be satisfied. From these three relations, the effects of variations in parts and tooling can be predicted.

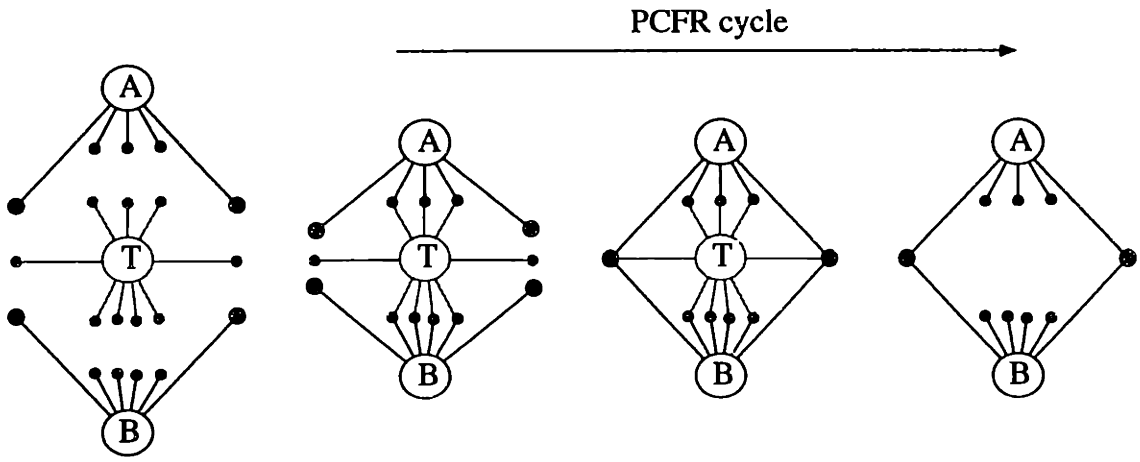

(a) before place (b) place/clamp (c) fasten (d) release

Figure 4.4 Graph representation of the PCFR cycle

4.3. Overview of simulation

Information required for simulation

The following information is required for the simulation of propagation of variations during the PCFR cycle:

- nominal position of features specified by the design (See section 3.1)
- number and type of mating features (See section 3.2)
- variations in parts and tooling (See section 3.3)
- constitutive relations of each part (See section 3.4)
- Contact chain: connections between mating pairs at each step of PCFR cycle (See section 4.2)

Modeling assumptions

The following assumptions are made to simplify the problem.

- Rigid, stationary assembly tooling: It is assumed that, unlike sheet metal parts, assembly tooling is rigid, and does not move during assembly.

- No friction: Friction forces are assumed to be negligible.

- Linearly isotropic elastic materials: Stress-strain relations are linear.

- Concentrated forces: It is assumed that external forces are applied only on mating features, and the forces can be approximated as concentrated loads.

- No melting and solidification of metal: Actual welding process includes local melting and solidification of metal. Modeling these phenomena is beyond the scope of this thesis.

Overview of simulation procedures

Due to the assumptions that friction can be neglected and the stress-strain relations are linear, the simulation can be reduced to two stages. In the first stage, the effects of the place, clamp, and fasten steps of the PCFR cycle are examined, and in the second stage, the variations that occur after the release step are calculated.

Procedure 1. Finding the location of actual welding spots: The inputs of this procedure are variations in parts and assembly tooling. The outputs of this procedure are the deviations of welding spots.

Procedure 2. Finding the actual positions and shapes of parts in the assembly: The inputs of this procedure are variations in parts and deviations of welding spots. The outputs of this step are the displacements and deformations of parts in the assembly.

4.4. Procedure 1: Finding deviations of welding spots

Take, for example, parts in a fixture just before welding guns pass electric currents; parts are placed and clamped in a fixture and then grasped by the welding guns. The displacements and deformations of the parts can be calculated from (1) the constitutive relations and (2) the geometric compatibility at the mating features.

Constitutive relations

As stated in section 3.4, the constitutive relations of each part can be represented in the form

$$\mathbf{f}_m = \mathbf{K}_m \mathbf{u}_m, \qquad \text{Eq. 3.12}$$

where $\mathbf{u}_m$ is the displacement vector of the mating features,

$$\mathbf{u}_m = \begin{Bmatrix} \upsilon_1 \\ \upsilon_2 \\ \vdots \\ \upsilon_i \\ \vdots \\ \upsilon_N \end{Bmatrix} \text{ (υ_i is the displacement of the i-th mating feature),} \qquad \text{Eq. 3.13}$$

$\mathbf{f}_m$ is the force vector acting on the mating features and $\mathbf{K}_m$ is the corresponding stiffness matrix.

Geometric compatibility at mating features

Ideally a pair of mating features should be at the same position, but due to variations in incoming parts and tooling and displacements and deformations of parts during assembly, the positions of two features differ from each other. The difference is constrained by the

allowable relative motion, λ, which is determined by the mating feature type[2]. This is illustrated in Figure 4.5.

In the figure, $\mathcal{A}.i$ and $\mathcal{B}.i$ are the coordinate frames of the mating features of parts A and B in their ideal positions, $\mathcal{A}.i'$ and $\mathcal{B}.i'$ are the coordinate frames deviating from the ideal positions due to variations in parts and tooling, and $\mathcal{A}.i''$ and $\mathcal{B}.i''$ are the coordinate frames at the actual feature positions due to further deviation during assembly.

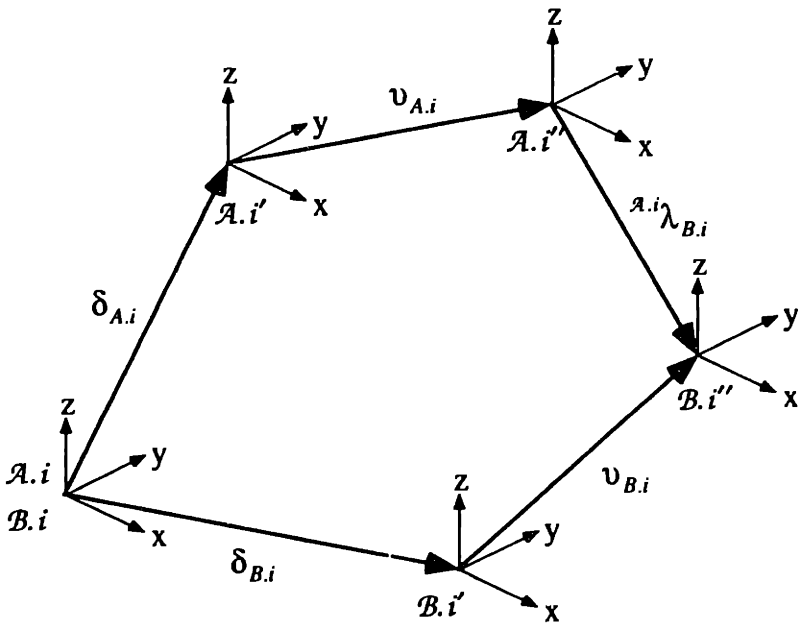

Figure 4.5. The closed loop of variations, displacements during assembly, and relative motion between a pair of mating features

Because δ's and υ's are small, the position of $\mathcal{B}.i''$ relative to $\mathcal{A}.i''$ is approximately[3]

$$^{\mathcal{A}.i}\lambda_{B.i} = -\upsilon_{A.i} - \delta_{A.i} + \delta_{B.i} + \upsilon_{B.i}. \qquad \text{Eq. 4.1}$$

As discussed in section 3.2, $^{\mathcal{A}.i}\lambda_{B.i}$ in Eq. 4.1 is constrained by the mating feature type. Table 4.1 lists geometric compatibility derived from Eq. 4.1 and constraints on $^{\mathcal{A}.i}\lambda_{B.i}$[4] for

[2]See section 3.2
[3]See Appendix E
[4]See section 3.2

various mating feature types. In the table, $A.i$ refers to a feature on a part, while $\underline{F.j}$ refers to the corresponding feature on its fixture. $\upsilon_{\underline{F.j}}$ is zero for all types of mating features because fixtures are assumed to be stationary during assembly.

Type	Geometric compatibility	Direction
Locator pin and hole	$\upsilon_{A.i,x} = \delta_{\underline{F.j,x}} - \delta_{A.i,x}$ $\upsilon_{A.i,y} = \delta_{\underline{F.j,y}} - \delta_{A.i,y}$	centerline is in the z-direction
Locator pin and slot	$\upsilon_{A.i,y} = \delta_{\underline{F.j,y}} - \delta_{A.i,y}$	centerline is in the z-direction and longer axis of the slot is in the x-direction
Locator block and surface	$\upsilon_{A.i,z} = \delta_{\underline{F.j,z}} - \delta_{A.i,z}$	normal vector of the surface is in the z-direction
Clamp and surface	$\upsilon_{A.i,z} = \delta_{\underline{F.j,z}} - \delta_{A.i,z}$ $\upsilon_{A.i,\psi} = \delta_{\underline{F.j,\psi}} - \delta_{A.i,\psi}$ $\upsilon_{A.i,\theta} = \delta_{\underline{F.j,\theta}} - \delta_{A.i,\theta}$	normal vector of the surface is in the z-direction
Welding gun and surface	$\upsilon_{A.i,z} = \delta_{\underline{F.j,z}} - \delta_{A.i,z}$ $\upsilon_{A.i,\psi} = \delta_{\underline{F.j,\psi}} - \delta_{A.i,\psi}$ $\upsilon_{A.i,\theta} = \delta_{\underline{F.j,\theta}} - \delta_{A.i,\theta}$	normal vector of the surface is in the z-direction

Table 4.1 Geometric compatibility at mating features

Deviations of welding spots

From the constitutive relations and the geometric compatibility discussed above, one can find the displacements of features on parts for given variations in parts and tooling. Let the displacements of the welding surfaces of part A and B during assembly be $\upsilon_{A.i}$ and $\upsilon_{B.i}$,

respectively. The next step is to relate the displacements of the features to the deviations of the welding spots.

Figure 4.6 illustrates the region where a welding gun touches two parts A and B. Dotted lines represent the objects in their ideal positions, while solid lines represent the objects in their actual positions. Hollow circles represent the positions on parts where they should be welded, while solid circles represent the positions on parts where they are actually welded. The differences between the ideal and the actual welding spots are the deviations of the welding spots, and are denoted by $\omega_{A.i}$ and $\omega_{B.i}$.

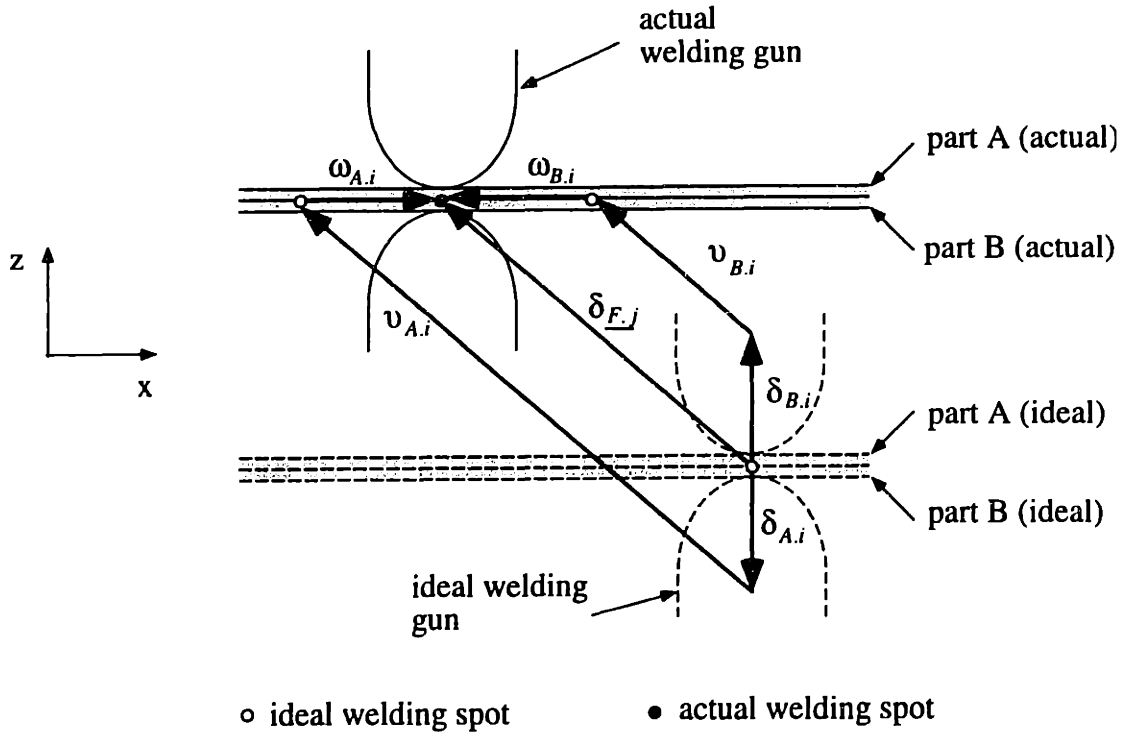

Figure 4.6 Deviations of welding spots

Deviations of welding spots are defined only in the directions tangential to the welding surfaces. As shown in Figure 4.6, the deviations of welding spots on part A and B in the x-direction are approximately,

$$\omega_{A.i,x} = -\upsilon_{A.i,x} - \delta_{A.i,x} + \delta_{\underline{F.j,x}},$$

$$\omega_{B.i,x} = -\upsilon_{B.i,x} - \delta_{B.i,x} + \delta_{\underline{F.j,x}}. \qquad \text{Eq. 4.2}$$

In a three-dimensional welding surface whose normal is in the z-direction, the deviations of the welding spots in the x and y-direction are

$$\omega_{A.i,x} = -\delta_{A.i,x} - \upsilon_{A.i,x} + \delta_{\underline{F.j,x}}$$

$$\omega_{A.i,y} = -\delta_{A.i,y} - \upsilon_{A.i,y} + \delta_{\underline{F.j,y}}. \qquad \text{Eq. 4.3}$$

4.5. Procedure 2: Finding variations in the assembly

The next step is to find variations in the resultant assembly with respect to its complete locator scheme[5]. Variations in the resultant assembly can be calculated from the constitutive relations, geometric compatibility, and force continuity.

Constitutive relations

The constitutive relations of each part are represented in the form

$$\mathbf{f}_m = \mathbf{K}_m \mathbf{u}_m, \qquad \text{Eq. 3.12}$$

where $\mathbf{u}_m$ is the displacement vector of the mating features,

$$\mathbf{u}_m = \begin{Bmatrix} \underline{\upsilon_1} \\ \underline{\upsilon_2} \\ \underline{\vdots} \\ \underline{\upsilon_i} \\ \underline{\vdots} \\ \underline{\upsilon_N} \end{Bmatrix} (\upsilon_i \text{ is the displacement of the } i\text{-th mating feature}), \qquad \text{Eq. 3.13}$$

[5]The complete locator scheme is defined in section 3.3

$\mathbf{f}_m$ is the force vector acting on the mating features and $\mathbf{K}_m$ is the corresponding stiffness matrix.

Geometric compatibility

Figure 4.7 illustrates geometric compatibility at welds. Dotted lines represent the ideal geometry of parts. Solid lines represent the actual geometry of parts. $\delta_{A.i}$ and $\delta_{B.i}$ are the variations in the welding surfaces of part A and B. $\upsilon_{A.i}$ and $\upsilon_{B.i}$ are the displacements of welding surface features in the assembly. $\omega_{A.i}$ and $\omega_{B.i}$ are the deviations of welding spots on the welding surfaces that are calculated in the previous step. From the condition that the weld joint on two parts should be at the same position in the assembly, we have the following equation:

$$\delta_{A.i} + \omega_{A.i} + \upsilon_{A.i} = \delta_{B.i} + \omega_{B.i} + \upsilon_{B.i}. \qquad \text{Eq. 4.4}$$

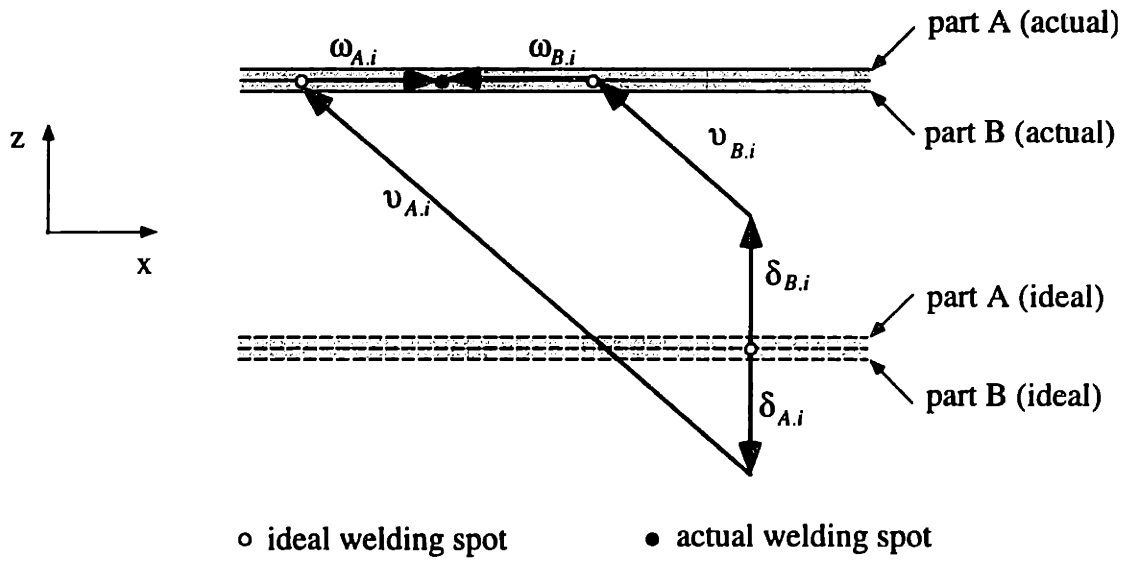

Figure 4.7 Geometric compatibility at weld joint

Geometric compatibility at mating features between parts and the locator scheme of the assembly is the same as in procedure 1.

Equations from force continuity

Because forces at the weld joint should be in equilibrium, we have the following equation at each weld joint:

$$\mathbf{f}_{A.i} + \mathbf{f}_{B.i} = 0 \qquad \text{Eq. 4.5}$$

where $\mathbf{f}_{A.i}$ and $\mathbf{f}_{B.i}$ are the forces at the weld joint on part A and B, respectively.

Solution

Displacements of mating features $\mathbf{u}_m$ and contact forces at weld $\mathbf{f}_{A.i}$ and $\mathbf{f}_{B.i}$ can be found from the constitutive relations in each part and from geometric compatibility and force continuity at each contact in contact chain. Then, the variations of a feature in the assembly δ_{Assy} is

$$\delta_{Assy} = \delta_{Part} + \upsilon \qquad \text{Eq. 4.6}$$

4.6. Simulation of multiple PCFR cycles

Simulation of a PCFR cycle is summarized in Figure 4.8. For given errors in parts and assembly tooling, assembly variations are calculated in the following procedures:

1. Deviation of welding spots are calculated from given errors.

2. Variations in assembly are then calculated.

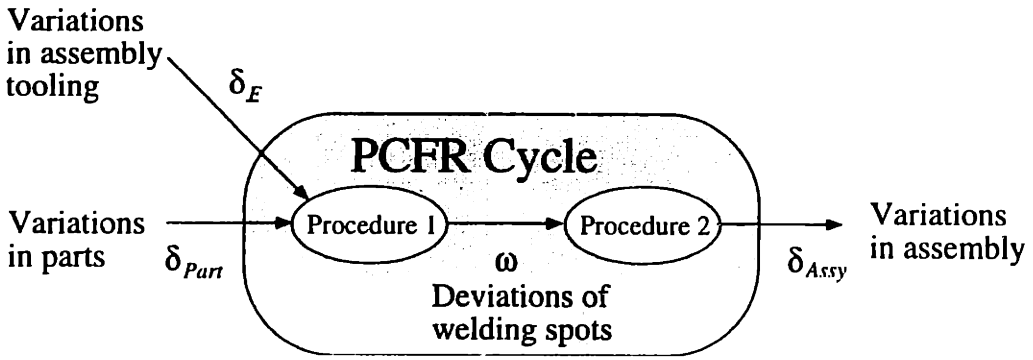

Figure 4.8 Simulation of a PCFR cycle: summary

The simulation method for a single PCFR cycle described in sections 4.4 and 4.5 can be generalized to the simulation of multiple PCFR cycles. This is schematically illustrated in Figure 4.9. Dimensional errors of a subassembly, δ_{Sassy}'s, are found from one simulation. This δ_{Sassy} is then the input of the next simulation. In this way we can simulate a number of PCFR cycles.

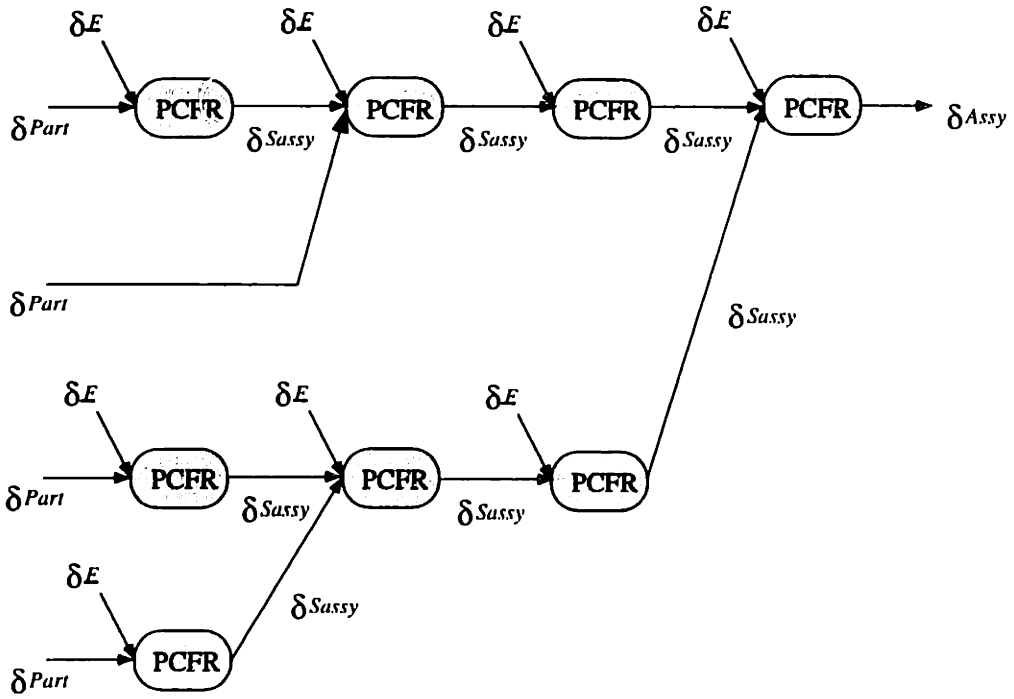

Figure 4.9 Simulation of multiple PCFR cycles

4.7. Summary

Key points discussed in this chapter can be summarized as

- The assembly process is modeled as a series of PCFR cycles.
- Contact chains are proposed to represent interactions between parts and tooling at each step of the PCFR cycle.
- Simulation procedures are developed to predict variations in the assembly from given variations in incoming parts and assembly tooling.

5

Validation

The assembly model described in chapter 4 is implemented and tested for assemblies of simple two dimensional parts. In two dimensional space, there are three degrees of freedom: two translations and one rotation. Thus, the displacements are represented by 3×1 vectors instead of 6×1 vectors. For example, dimensional error of a feature is

$$\delta_{A.i} = \left\{\delta_x,\ \delta_y,\ \delta_\theta\right\}^T. \qquad \text{Eq. 5.1}$$

where δ_x and δ_y are the translational errors in the x and y-direction respectively, and δ_θ is the rotational error around the axis into the paper (Figure 5.1).

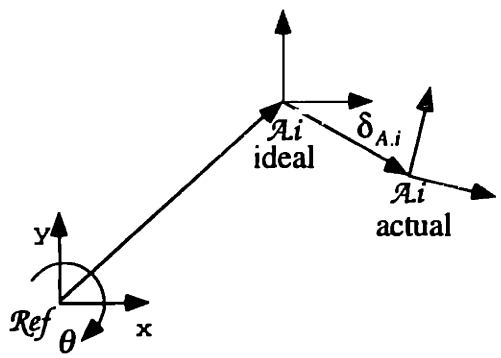

Figure 5.1. Variations in two dimensional space

Likewise, the displacement of a feature during assembly and the relative motion between features are represented by 3×1 vectors as in Eq. 5.2.

$$\upsilon_{A.i} = \left\{ \upsilon_x,\ \upsilon_y,\ \upsilon_\theta \right\}^T$$

$$^{B.i}\lambda_{A.i} = \left\{ \lambda_x,\ \lambda_y,\ \lambda_\theta \right\}^T \qquad \text{Eq. 5.2}$$

To obtain the constitutive relations of parts, the following assumptions are made.

- Parts are modeled as assemblies of Hermite cubic Euler-Bernoulli beam elements [Reddy 93] with the same material properties and thicknesses.
- The stiffness corresponding to axial displacement is assumed to be much larger than the stiffness corresponding to transverse displacement.
- Joints between beam elements are assumed to be rigid, i.e., joint angles do not change under loading.

Five types of two dimensional contacts are used in the examples: pin/hole, block/surface, clamp/surface, welding gun/surface, and welded joint. The geometric compatibility at these contacts are listed in Table 5.1.

The following three examples will be provided in this chapter.

(1) The effects of variations in parts and tooling on an assembly consisting of two parts welded at one point (Section 5.1)

(2) The effects of variations in parts on an assembly consisting of two parts welded at two points (Section 5.2)

(3) The effects of variations in parts on an assembly consisting of three parts assembled through two PCFR cycles (Section 5.3)

Type	Geometric compatibility	Direction
Locator pin and hole	$\delta_{A.i,x} + \upsilon_{A.i,x} = \delta_{\underline{F.j,x}}$	centerline is in the y-direction
Locator block and surface	$\delta_{A.i,y} + \upsilon_{A.i,y} = \delta_{\underline{F.j,y}}$	normal vector of the surface is in the y-direction
Clamp and surface	$\delta_{A.i,y} + \upsilon_{A.i,y} = \delta_{\underline{F.j,y}}$ $\delta_{A.i,\theta} + \upsilon_{A.i,\theta} = \delta_{\underline{F.j,\theta}}$	normal vector of the surface is in the y-direction
Welding gun and surface	$\delta_{A.i,x} + \upsilon_{A.i,x} = \delta_{\underline{F.j,x}}$ $\delta_{A.i,\theta} + \upsilon_{A.i,\theta} = \delta_{\underline{F.j,\theta}}$	normal vector of the surface is in the x-direction
Welded joint	$\delta_{A.i,x} + \upsilon_{A.i,x} = \delta_{B.i,x} + \upsilon_{B.i,x}$ $\delta_{A.i,y} + \upsilon_{A.i,y} = \delta_{B.i,y} + \upsilon_{B.i,y}$ $\delta_{A.i,\theta} + \upsilon_{A.i,\theta} = \delta_{B.i,\theta} + \upsilon_{B.i,\theta}$	any directions

Table 5.1 Geometric compatibility at two dimensional mating features

5.1. Example 1. Assembly with one weld joint

The model shown in Figure 5.2 illustrates the assembly of two parts. Part *A* and *B* in Figure 5.2 (a) are placed, clamped, and welded as shown in Figure 5.2 (b). After the assembly is released, assembly variations are measured with respect to the locating scheme shown in Figure 5.2 (c).

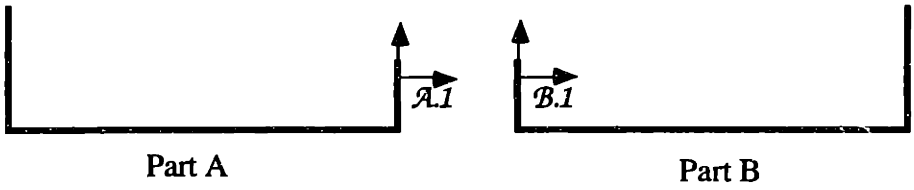

(a) Parts and mating features

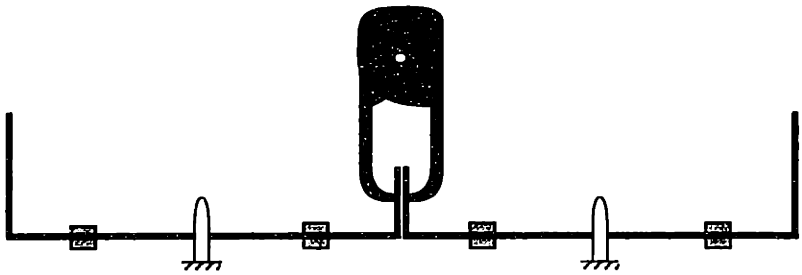

(b) Parts and assembly tooling

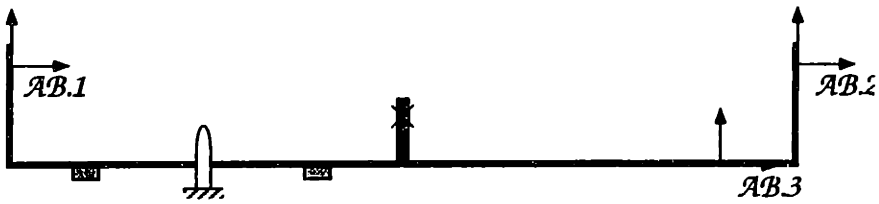

(c) Resultant assembly and its locating scheme

Figure 5.2 Two dimensional assembly consisting of two parts

5.1.1. Effects of variations in parts

Suppose that the welding surface of part A, i.e., $A.1$ in Figure 5.2 (a), has a variation as represented in Eq. 5.3, while the rest of dimensions, in both parts and tooling, are perfect.

$$\delta_{A.1} = \{-\Delta_x,\ 0,\ 0\}^T, \qquad \text{Eq. 5.3}$$

When the parts are placed and clamped in a fixture, there is a gap between the two welding surfaces as shown in Figure 5.3 (a) because of the variation in the welding surface. During fastening, a welding gun closes the gap by pulling part A with its fingers

as illustrated in Figure 5.3 (b). As a result, the actual welding spot on part A differs from where it should be due to the deformation of part A. The spots that the finger tips touch are then welded. When the assembly is released from the fixture, the parts spring back as shown in Figure 5.3 (c).

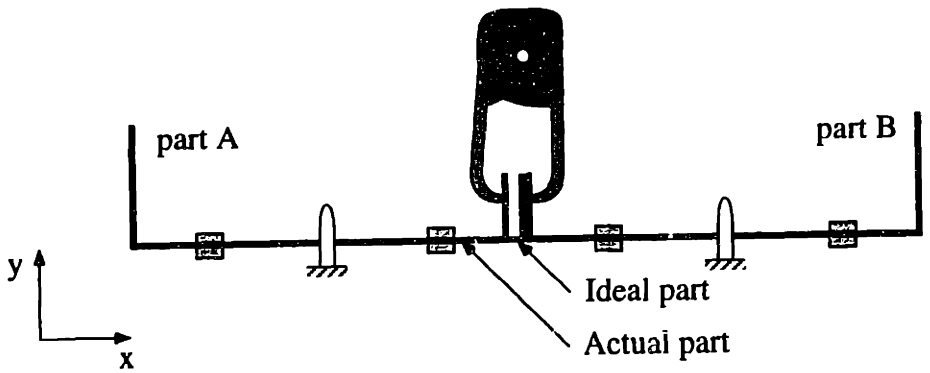

(a) After parts are placed and clamped

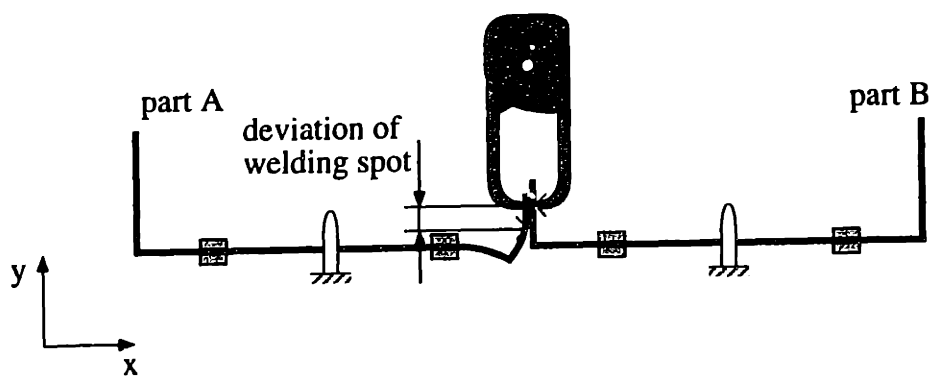

(b) Deviations of welding spots during fastening

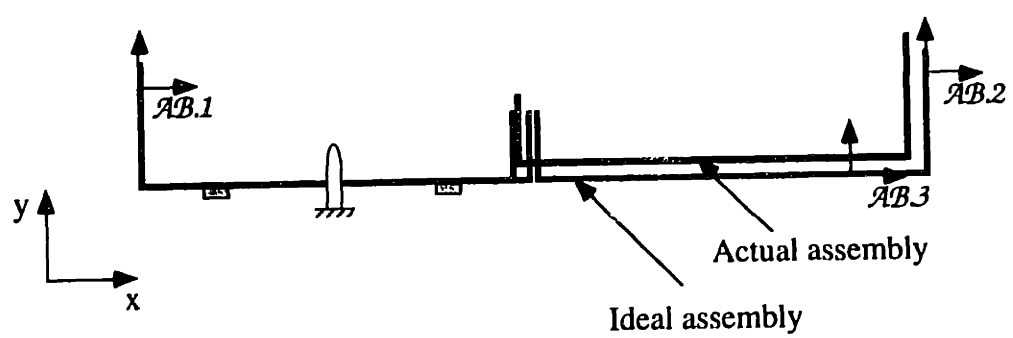

(c) Variations in the resultant assembly

Figure 5.3 Effects of variations in parts

A close-up of the welding surface of part A during fastening is illustrated in Figure 5.4. When a force F and a moment M are applied to the welding surface of part A, the deformation of the welding point is approximately

$$\upsilon_{A.1} = \left\{ b\theta_1 + u_x \quad u_y \quad \theta_1 + \theta_2 \right\}^T. \qquad \text{Eq. 5.4}$$

where

$$u_x = \frac{Fb^3}{3EI} + \frac{Mb^2}{2EI},\ u_y = -\frac{M + bF}{2EI}a^2$$

$$\theta_1 = \frac{M + bF}{EI}a, \text{ and } \theta_2 = \frac{Fb^2}{2EI} + \frac{Mb^2}{EI}. \qquad \text{Eq. 5.5}$$

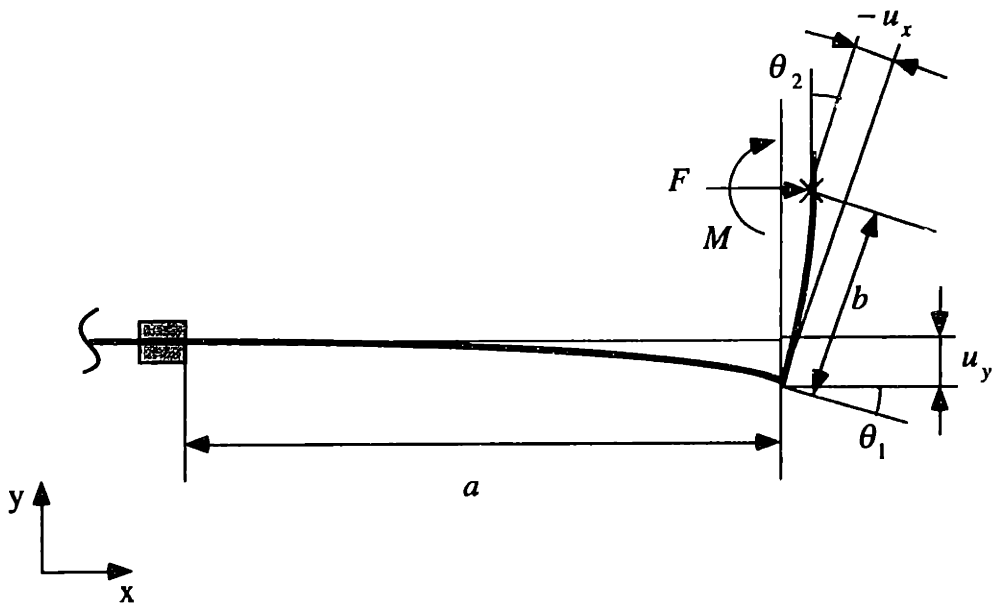

Figure 5.4 Close-up of the welding surface of part A during fastening

From geometric compatibility at the contact between the welding gun and welding surface,

$$\upsilon_{A.1,x} = b\theta_1 + u_x = \Delta_x, \text{ and}$$

$$\upsilon_{A.1,\theta} = \theta_1 + \theta_2 = 0. \qquad \text{Eq. 5.6}$$

From Eq. 5.5 and Eq. 5.6, Eq. 5.4 can be rewritten as

$$\upsilon_{A.1} = \left\{ \Delta_x \quad \frac{-3a^2}{(4a+b)b}\Delta_x \quad 0 \right\}^T . \qquad \text{Eq. 5.7}$$

Therefore, the difference between the actual and ideal welding spot on part A is

$$\omega_{A.1,y} = -\upsilon_{A.1,y} = \frac{3a^2}{(4a+b)b}\Delta_x . \qquad \text{Eq. 5.8}$$

When the assembly is released, variations of features $AB.1$, $AB.2$, and $AB.3$ in Figure 5.3 (c) are

$$\delta_{AB.1} = \{0,\ 0,\ 0\}^T ,$$

$$\delta_{AB.2} = \{-\Delta_x,\ 0,\ 0\}^T \text{[1]}, \text{ and}$$

$$\delta_{AB.3} = \left\{ 0,\ \frac{3a^2}{(4a+b)b}\Delta_x,\ 0 \right\}^T \text{[2]}. \qquad \text{Eq. 5.9}$$

If $a = 100$ and $b = 50$, the variation of $AB.3$ is

$$\delta_{AB.3} = \{0,\ 1.3\Delta_x,\ 0\}^T . \qquad \text{Eq. 5.10}$$

Note that the variation in feature $A.1$ is amplified by a factor of 1.3 in feature $AB.3$.

5.1.2. Effect of variations in locator pins

Suppose that incoming parts are perfect but the locator pin for part A has a variation as given in Eq. 5.11.

$$\delta = \{-\Delta_x,\ 0,\ 0\}^T . \qquad \text{Eq. 5.11}$$

---

[1]Variation in the y-direction is zero because variations are not defined in the direction normal to the surface.
[2]Variation in the x-direction is zero because variations are not defined in the direction normal to the surface.

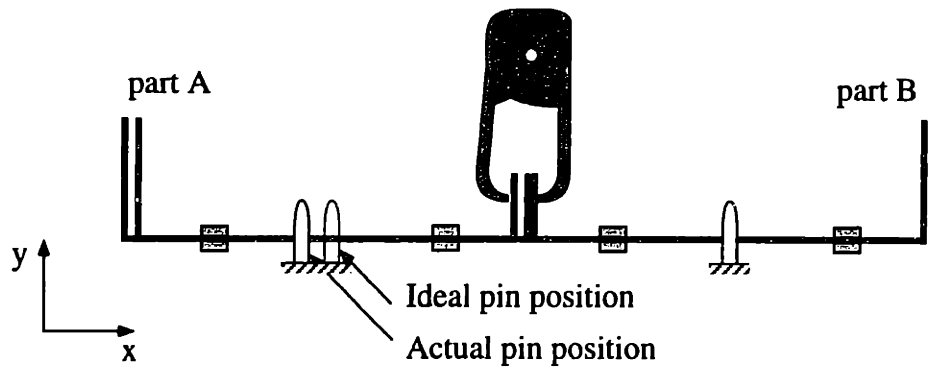

(a) Dimensional error in locator pin position

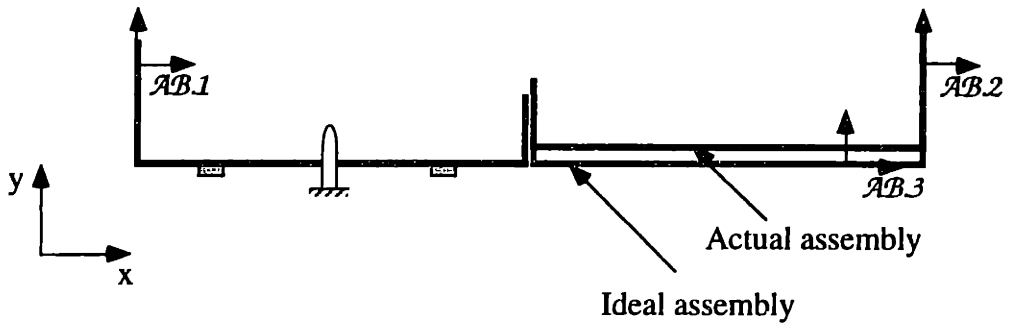

(b) Variations in the resultant assembly

Figure 5.5 Effects of variation in locator pins

When the ideal parts are placed in the imperfect fixture, part A is shifted in the negative y-direction. As a result, there is a gap between the two welding surfaces as shown in Figure 5.5 (a). This situation is very similar to the case in section 5.1.1; the welding gun pulls part A, and as a result, welding spots change. When the assembly is released, the variations of features $AB.1$, $AB.2$, and $AB.3$ in Figure 5.5 (b) are

$$\delta_{AB.1} = \{0,\ 0,\ 0\}^T,$$

$$\delta_{AB.2} = \{0,\ 0,\ 0\}^T, \text{ and}$$

$$\delta_{AB.3} = \left\{0,\ \frac{3a^2}{(4a+b)b}\Delta_x,\ 0\right\}^T. \qquad \text{Eq. 5.12}$$

5.1.3. Effect of variations in locator blocks/clamps

Suppose that incoming parts and locator pins are perfect but the clamp for part A in the right hand side has a variation as given in Eq. 5.13 (See Figure 5.6).

$$\delta = \{0,\ -\Delta_y,\ 0\}^T. \qquad \text{Eq. 5.13}$$

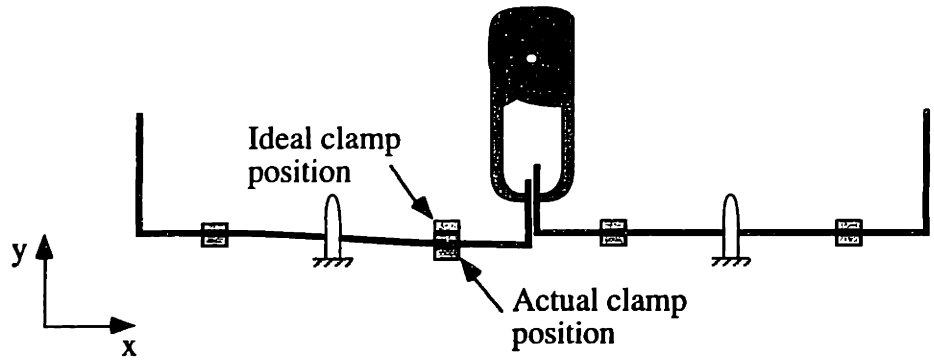

(a) Dimensional error in a clamp position

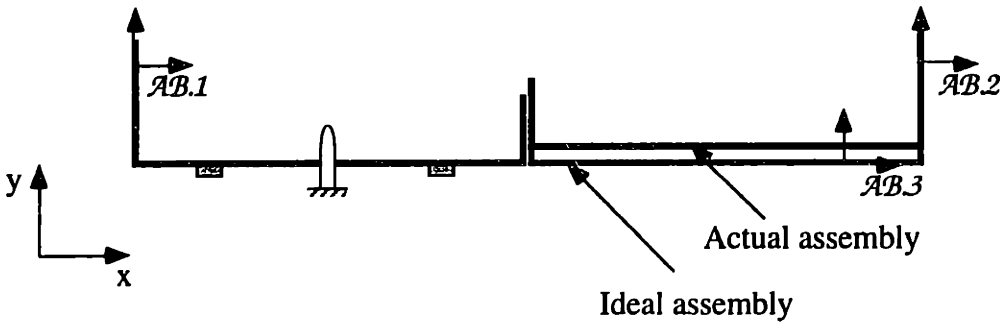

(b) Variations in the resultant assembly

Figure 5.6 Effects of variations in locator blocks/clamps

When the ideal parts are placed in the imperfect fixture, part A rotates from its ideal position. During clamping, clamps deform the part as shown in Figure 5.6 (a). As a result, the welding surface of part A moves by $-\Delta_y$ in the y-direction. As the welding surface is moved by $-\Delta_y$, the actual welding spot on part A differs from its ideal position by Δ_y. When the assembly is released, the variations of features $AB.1$, $AB.2$, and $AB.3$ in Figure 5.6 (b) are

$$\delta_{AB.1} = \{0,\ 0,\ 0\}^T,$$

$$\delta_{AB.2} = \{0,\ 0,\ 0\}^T$$[3], and

$$\delta_{AB.3} = \{0,\ \Delta_x,\ 0\}^T. \qquad \text{Eq. 5.14}$$

5.1.4. Effect of variations in welding guns

Finally, suppose that incoming parts and fixtures are perfect but the welding gun is trying to weld in a position that differs from the nominal by

$$\delta = \{\Delta_x,\ 0,\ 0\}^T. \qquad \text{Eq. 5.15}$$

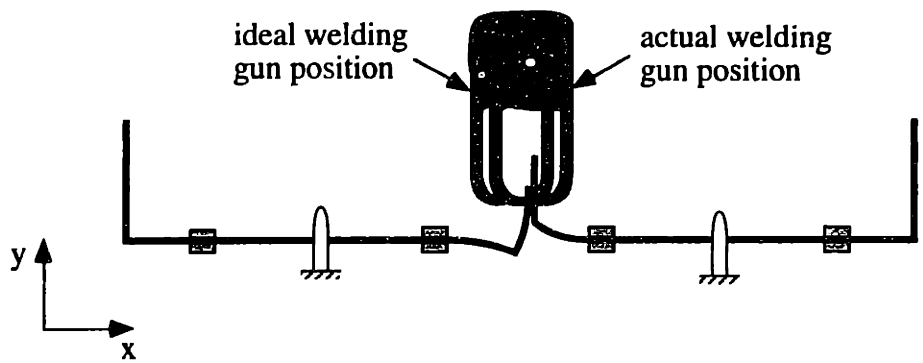

(a) Dimensional errors of welding gun position

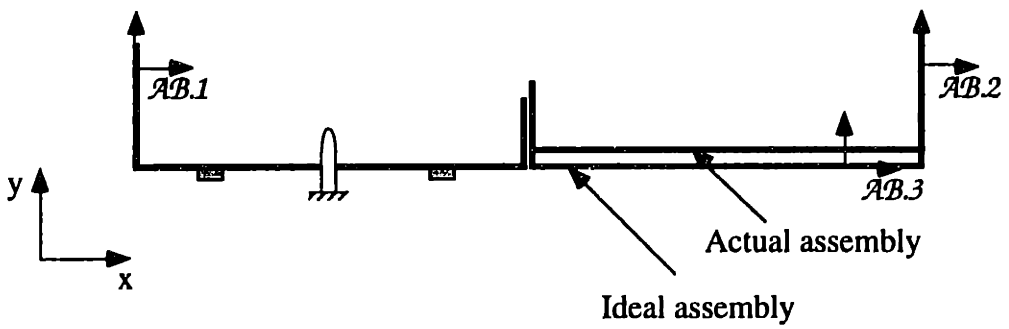

(b) Variations in the resultant assembly

Figure 5.7 Effects of variations in welding guns

[3]Variation in the y-direction is zero because variations are not defined in the direction normal to the surface.

Until the parts are placed and clamped in the fixture, parts do not deform. During fastening, however, the welding gun pulls the welding surfaces of part A and B by Δ_x in the x-direction as shown in Figure 5.7 (a). Suppose part A and B have the same dimensions, then the welding spots on both part A and B change by

$$\omega_{A.1,y} = \frac{3a^2}{(4a+b)b}\Delta_x \qquad \text{Eq. 5.16}$$

and

$$\omega_{B.1,y} = -\frac{3a^2}{(4a+b)b}\Delta_x. \qquad \text{Eq. 5.17}$$

When the assembly is released, the dimensional errors of features $AB.1$, $AB.2$, and $AB.3$ in Figure 5.7 (b) are

$$\delta_{AB.1} = \{0,\ 0,\ 0\}^T,$$

$$\delta_{AB.2} = \{0,\ 0,\ 0\}^T, \text{ and}$$

$$\delta_{AB.3} = \left\{0,\ \frac{6a^2}{(4a+b)b}\Delta_x,\ 0\right\}^T. \qquad \text{Eq. 5.18}$$

5.2. Example 2. Assembly with two weld joints

The assembly shown in Figure 5.8 requires welding on both side. Because part positions in the resultant assembly are over-constrained by two weld joints, parts may remain deformed in the assembly, even after the assembly is released from the fixture.

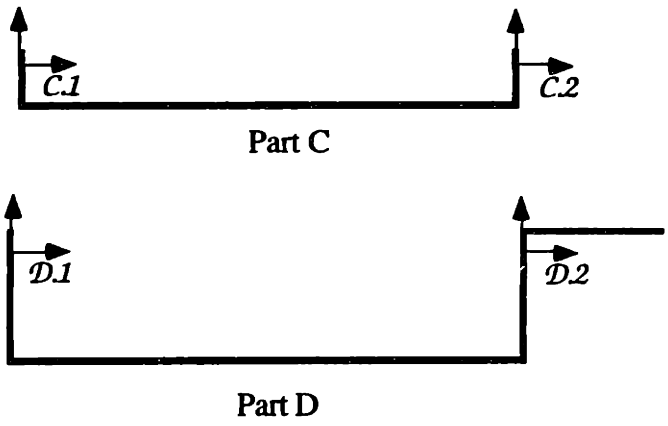

(a) Parts and mating features

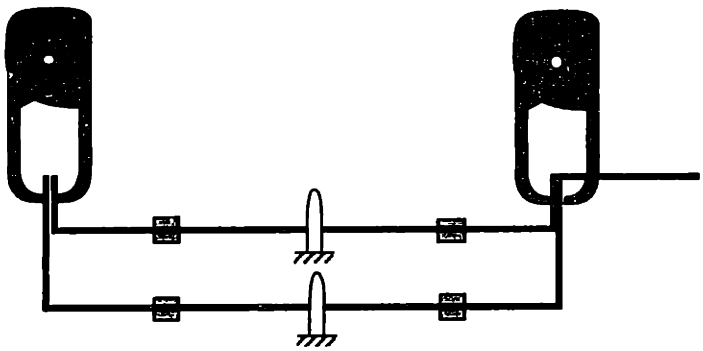

(b) Parts and assembly tooling

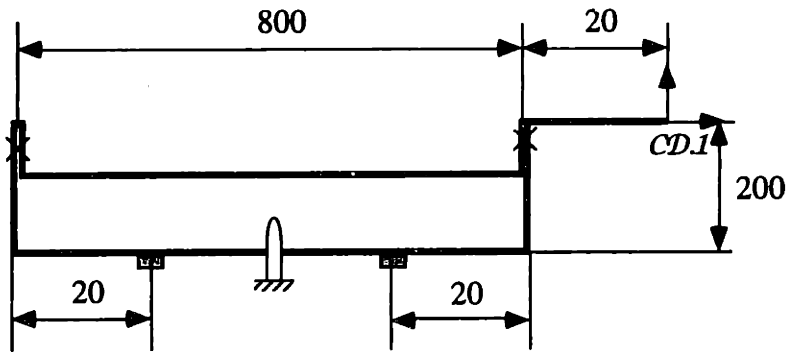

(c) Resultant assembly and its locating scheme

Figure 5.8 Assembly with multiple welds

Suppose that the right hand side welding surface of part C, i.e., $C.2$, has a variation as given in Eq. 5.19 while the rest of dimensions, in both parts and tooling, are perfect (See Figure 5.9).

$$\delta_{C.2} = \{-1,\ 0,\ 0\}^T, \qquad \text{Eq. 5.19}$$

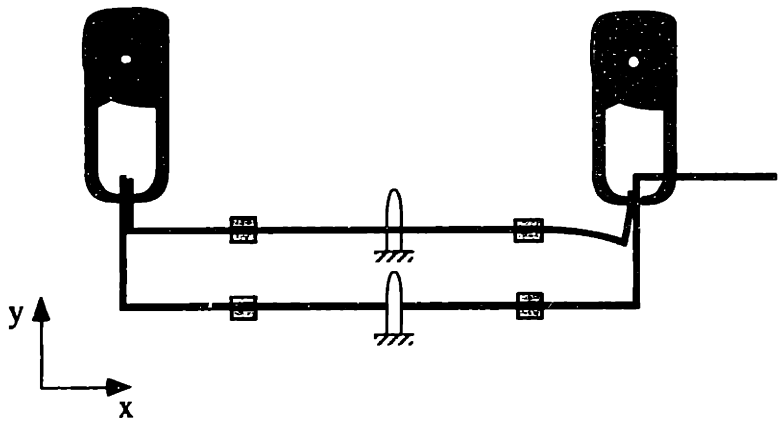

(a) Deformation of parts during fastening

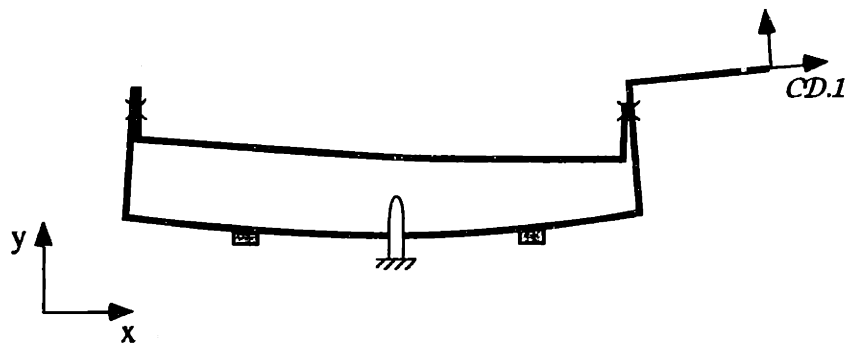

(b) Variations in the resultant assembly

Figure 5.9 Effects of variations when an assembly has locked-up stresses

When the parts are placed, clamped, and fastened as illustrated in Figure 5.9 (a), the actual welding spot on the right hand side of part C differs from its ideal position because of the same reason discussed in section 5.1.1. When the assembly is released from the fixture, the parts spring back as shown in Figure 5.9 (b). Because the parts are welded at

two points, the parts remain deformed in the assembly. The assembly is then released from the fixture.

The assembly variations are calculated from force continuity, geometric compatibility, and the constitutive relations. Solving these equations manually, as done in sections 5.1., is cumbersome. So, a finite element model is used to obtain a stiffness matrix. The variation of feature *CD*.1 is found to be:

$$\delta_{CD.1} = \{-1.3,\ 2.1,\ -0.4\}^T. \qquad \text{Eq. 5.20}$$

Note in Eq. 5.20 that a variation in the part is amplified in the assembly by factors as big as 2.1.

5.3. Example 3. Assembly through multiple PCFR cycles

The model shown in Figure 5.10 illustrates an assembly consisting of three parts that are assembled through two PCFR cycles. Part A and B are assembled first in the same manner described in section 5.1. Then part D is assembled to the sub-assembly AB, in the same manner described in section 5.2.

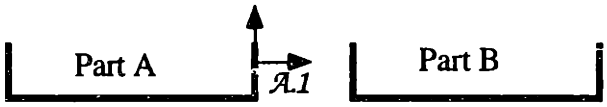

(a) Incoming parts for the first PCFR cycle

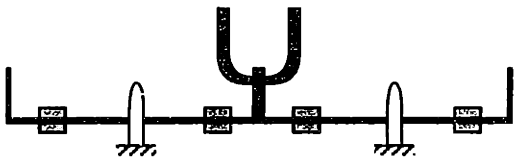

(b) The first PCFR cycle

Sub-assembly AB

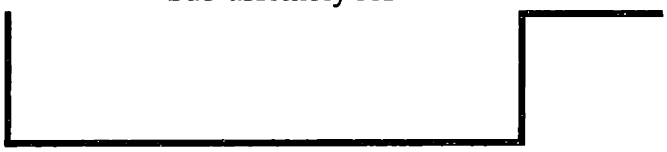

Part D

(c) Incoming part and sub-assembly for the second PCFR cycle

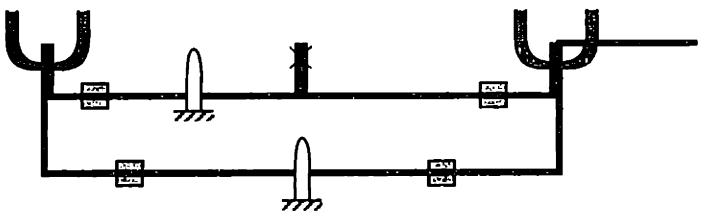

(d) The second PCFR cycle

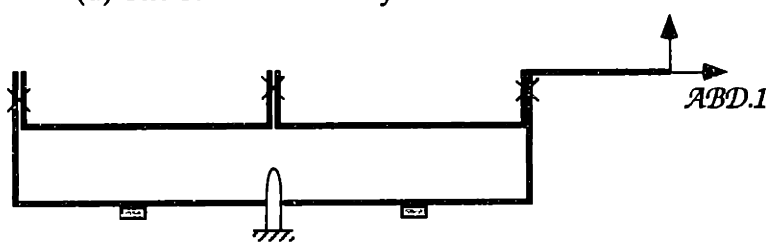

(e) Resultant assembly and its locating scheme

Figure 5.10 Two dimensional assembly consisting of three parts

Suppose that the welding surface of part A has a variation as given in Eq. 5.21, while the rest of dimensions, in both parts and tooling, are perfect.

$$\delta = \{-1,\ 0,\ 0\}^T, \qquad \text{Eq. 5.21}$$

Variations of sub-assembly AB are given in section 5.1. If $a = 100$ and $b = 50$, the variations of features $AB.1$, $AB.2$, and $AB.3$ are

$$\delta_{AB.1} = \{0,\ 0,\ 0\}^T,$$

$$\delta_{AB.2} = \{-1,\ 0,\ 0\}^T,$$

and

$$\delta_{AB.3} = \{0,\ 1.3,\ 0\}^T. \qquad \text{Eq. 5.22}$$

When the sub-assembly AB with its dimensional errors is assembled to part D, the clamp pushes sub-assembly AB because $\delta_{AB.3,y}$ is non-zero, and the welding gun pulls sub-assembly AB because $\delta_{AB.2,x}$ is non-zero. If dimensions of parts and tooling are as given in section 5.2, the dimensional error of feature $ABD.1$ is approximately

$$\delta_{CD.1} = \{-1.6,\ 2.6,\ -0.5\}^T. \qquad \text{Eq. 5.23}$$

Note in Eq. 5.23 that a variation in the part is amplified by factors as big as 2.6 in the assembly.

5.4. Summary

The work described in this chapter may be summarized as follows.

- The assembly model discussed in chapter 4 is implemented and tested for several two dimensional assemblies.

- The effects of variations in parts and tooling on the resultant assembly are studied.

An interesting discovery from this exercise is that sometimes variations in parts and tooling can be amplified through the PCFR cycle because of part deformations. Thus, we can say that part deformations during assembly cannot be neglected.

6
Applications

The assembly model proposed in chapter 5 is used for the following applications.

- Identification of critical dimensions (Section 6.1)
- Evaluation of robustness of design to variations (Section 6.2)
- Diagnosis of variation-related assembly problems (Section 6.3 through 6.8)

6.1. Identification of critical dimensions

Dimensions in parts and assembly tooling that are critical to an assembly can be found by evaluating the impacts of small changes in those dimensions on the critical dimensions of the assembly, i.e., sensitivity analysis. The sensitivities tells us which dimensions need to be monitored (1) to control the assembly process during production and also (2) to focus on improving the design[1]. This section describes the results of sensitivity analysis performed for an automobile front-end assembly.

[1] within the context of Taguchi's robust design [Taguchi 89].

6.1.1. The assembly

An automobile front-end assembly (structural part) is illustrated in Figure 6.1. The assembly consists of four major subassemblies: the radiator support, two inner fenders (left and right), and the body frame.

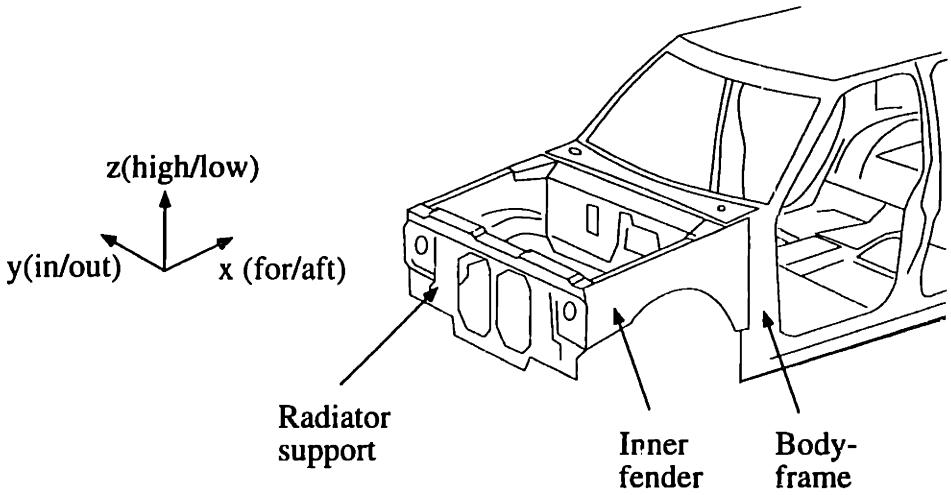

Figure 6.1 Front-end assembly

Simplified front-end assembly

For the purpose of simplicity, the front-end assembly is modeled as two-dimensional frames as shown in Figure 6.2.

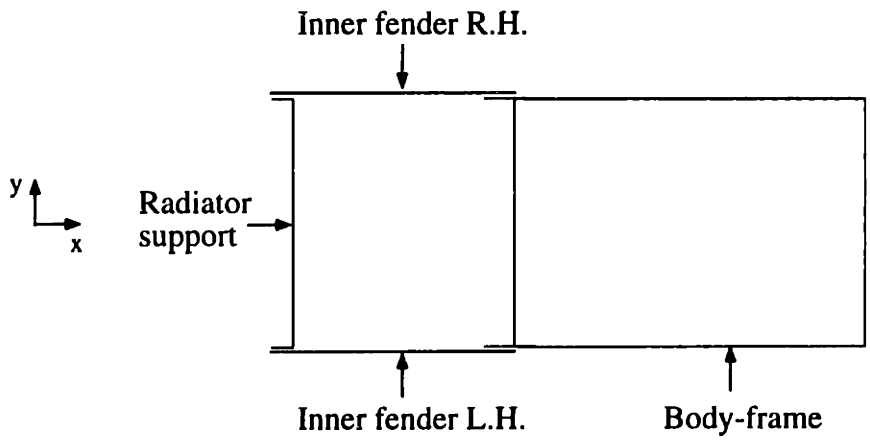

Figure 6.2 Simplified front-end assembly

6.1.2. Measuring points

Figure 6.3 illustrates some of the points that are measured to check the dimensions of the assembly. For/aft, i.e., x-directional, locations are measured at point m_1 and m_2, and in/out, i.e., y-directional, locations are measured at points m_3, m_4, m_5, and m_6.

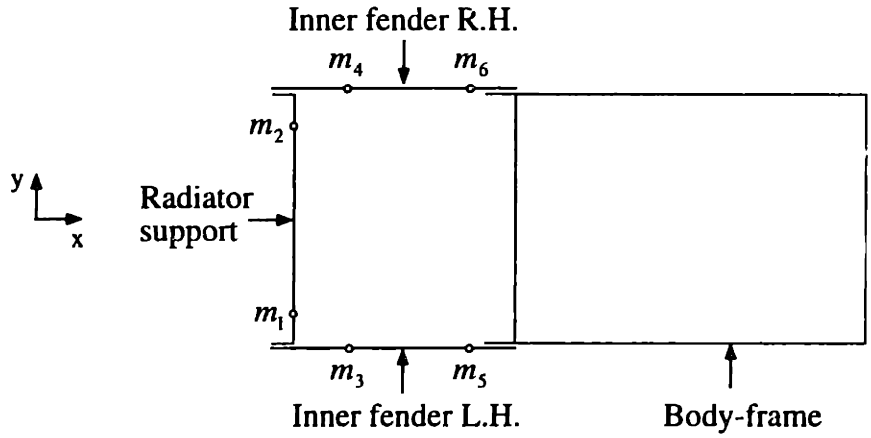

Figure 6.3 Measuring points on the front-end assembly

6.1.3. Mating features

There are forty-eight mating features in parts and tooling as illustrated in Figure 6.4; four part/part surface mates, five pin/hole mates, ten clamp/surface mates, and four welding gun/surface mates. Each mate has two mating features.

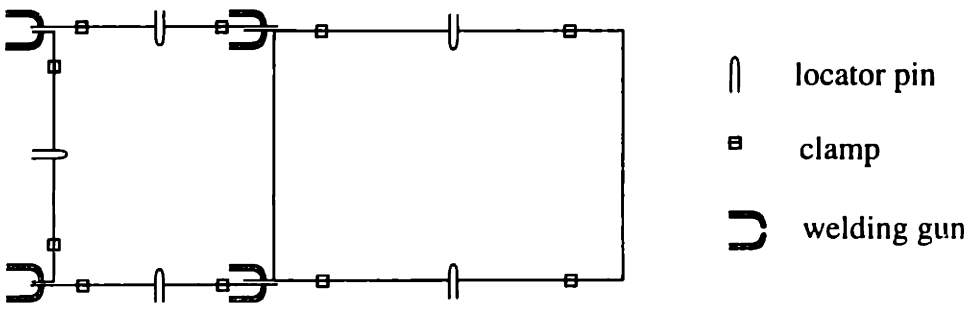

Figure 6.4 Mating features in the front-end assembly

6.1.4. Identified critical dimensions and their sensitivities

For each mating feature, sensitivities of the measuring points given in section 6.1.2. are evaluated. Figure 6.5 shows the mating features that are found to be critical, and Table 6.1 lists their sensitivities.

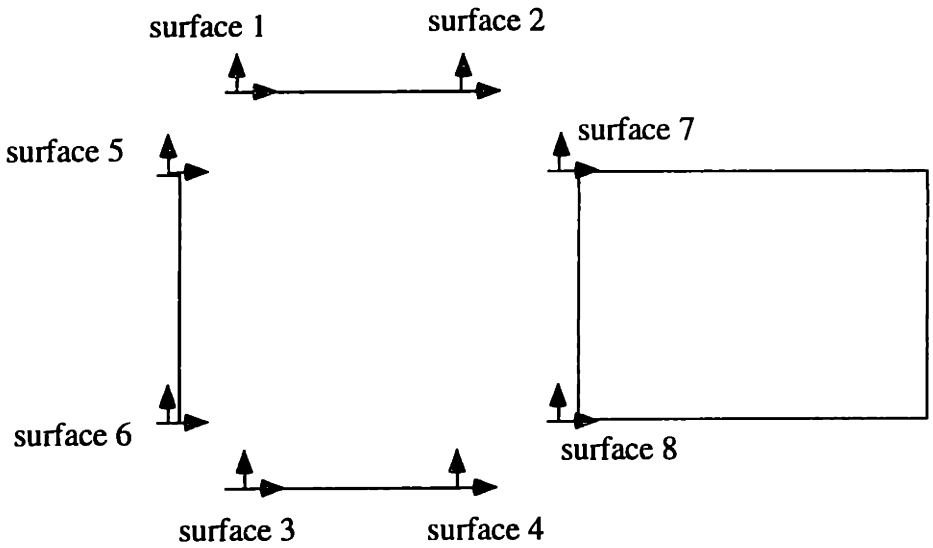

(a) critical features in parts

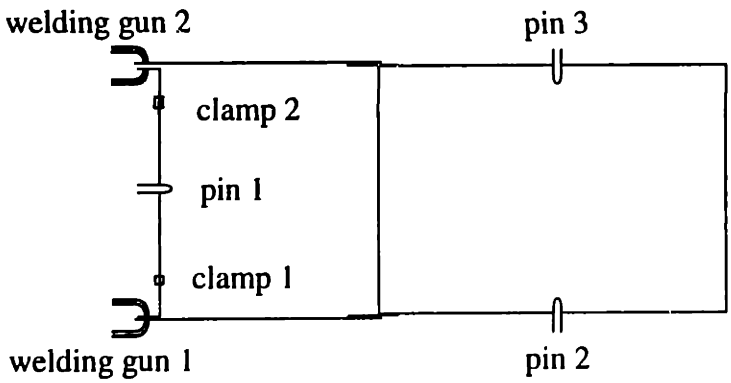

(b) critical features in tooling

Figure 6.5 Critical features for the front-end assembly

Critical Dimensions (unit: mm for location, and degree for orientation)	Sensitivities (unit: mm/mm or mm/degree)					
	$m_1(x)$	$m_2(x)$	$m_3(y)$	$m_4(y)$	$m_5(y)$	$m_6(y)$
1. clamp 1 location (x)	0.9	0.2	-0.2	-0.2	0.0	0.0
2. clamp 2 location (x)	0.2	0.9	0.2	0.2	0.0	0.0
3. welding gun 1 location (y)	-3.9	-0.7	1.0	0.9	0.1	0.1
4. welding gun 2 location (y)	0.7	3.9	0.9	1.0	0.1	0.1
5. surface 1 location (y)	0.0	0.0	0.4	0.4	0.1	0.1
6. surface 2 location (y)	0.0	0.0	-0.4	-0.4	-0.1	-0.1
7. surface 3 location (y)	0.0	0.0	0.4	0.4	0.1	0.1
8. surface 4 location (y)	0.0	0.0	-0.4	-0.4	-0.1	-0.1
9. surface 5 location (y)	-0.7	-3.9	-0.5	-1.4	0.0	-0.2
10. surface 6 location (y)	3.9	0.7	-1.4	-0.5	-0.2	0.0
11. surface 7 location (y)	0.0	0.0	0.1	0.1	0.4	-0.4
12. surface 8 location (y)	0.0	0.0	0.1	0.1	0.4	-0.4
13. pin 1 location (y)	3.2	-3.2	-1.9	-1.9	-0.2	-0.2
14. pin 2 location (x)	-0.85	-0.15	0.2	0.2	0.0	0.0
15. pin 3 location (x)	-0.15	-0.15	-0.2	-0.2	0.0	0.0
16. surface 5 orientation (θ)	0.0	0.0	3.7	1.3	0.8	-0.1
17. surface 6 orientation (θ)	0.0	0.0	1.3	3.7	-0.1	0.8
18. surface 7 orientation (θ)	0.0	0.0	3.7	4.4	0.8	3.2
19. surface 8 orientation (θ)	0.0	0.0	4.4	3.7	3.2	0.8

Table 6.1 The results of sensitivity analysis

6.2. Evaluation of robustness of design

One of the criteria for a good design is whether the design is robust to variations in the parts and tooling, i.e., how sensitive the final assembly is to variations in the parts and tooling. The results of sensitivity analysis will provide a rationale for comparing design alternatives of the product, assembly process, and assembly tooling. Generally speaking, a design with fewer critical dimensions that are sensitive to dimensions that customers care about is preferred. Figure 6.6 illustrates two alternatives for the assembly tooling design.

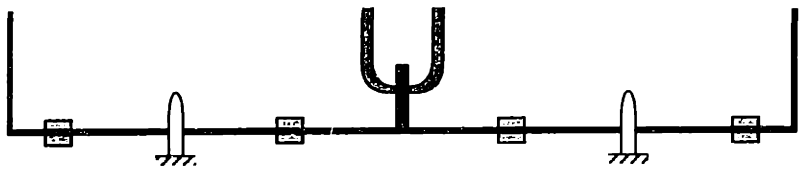

(a) Alternative 1

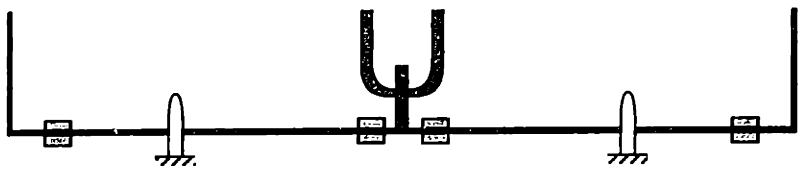

(b) Alternative 2

Figure 6.6 Assembly tooling design alternatives

The two design alternatives in Figure 6.6 are identical except for the positions of clamps near the welding surfaces. As shown in Eqs. 5.9, 5.12, and 5.18, the closer the clamps are to the welding surfaces, the lower is the sensitivity of the assembly to variations in welding surface, locator pin, and welding gun positions. Therefore, the second design alternative is better than the first design alternative from the point of robustness of design.

Now let us compare the designs in Figure 6.6 and the design in Figure 6.7. The welding surfaces in Figure 6.7 are horizontal while the welding surfaces in Figure 6.6 are

vertical[2]. Sensitivity analysis shows that the design shown in Figure 6.7 is even better because the assembly is almost independent of the variations in clamp and welding gun positions.

Figure 6.7 Product design alternative: assembly with a lap joint

Figures 6.8 (b) and (c) illustrate two assembly sequence alternatives for the assembly shown in Figure 6.8 (a). Parts A and B are assembled first, and then part C is added in Figure 6.8 (b). In Figure 6.8 (c), on the other hand, parts A and C, and parts B and C are welded first, and then parts A and B are welded together. For the sake of discussion, let us assume that the width of the assembly is important. Sensitivity analysis shows that the width of the assembly is less sensitive to variations in parts and tooling when the assembly is assembled through the sequence shown in Figure 6.8 (c).

[2]The welds shown in Figure 6.6 are called butt joints while the weld shown in Figure 6.7 is called a lap joint.

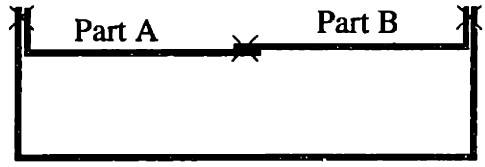

Part C

(a) The assembly

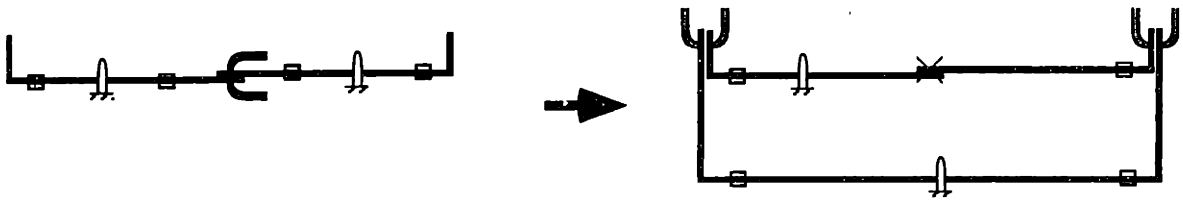

(b) Assembly sequence alternative 1

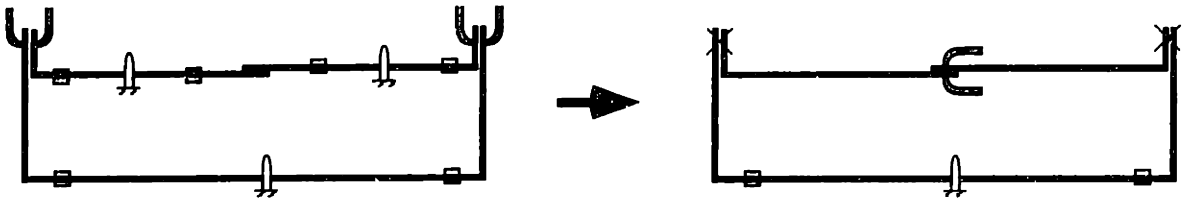

(c) Assembly sequence alternative 2

Figure 6.8 Assembly sequence alternatives

6.3. Diagnosis of assembly problems

So far, methods have been explained to identify the critical dimensions in parts and tooling and their first order relations to the variations in the measuring points (Section 6.1.) This relation has been used to evaluate design and assembly sequence alternatives (Section 6.2.) The rest of this chapter describes methods that use the relations to identify the cause(s) when the assembly has variation-related problems, i.e., when problems actually occur.

6.3.1. Diagnostic problem solving process

Once major subassemblies, e.g., door assembly and body panels, are assembled, their dimensions are measured at the specified points. If the measurement data deviate more than tolerable limits, it is brought to attention of the launch team. Launch team is a cross-organization team whose job is to explain why such problems are present. Typical launch team consists of people from various organizations: design team, part suppliers, assembly tooling suppliers, assembly plant, etc. Diagnosis problem solving process is illustrated in Figure 6.9.

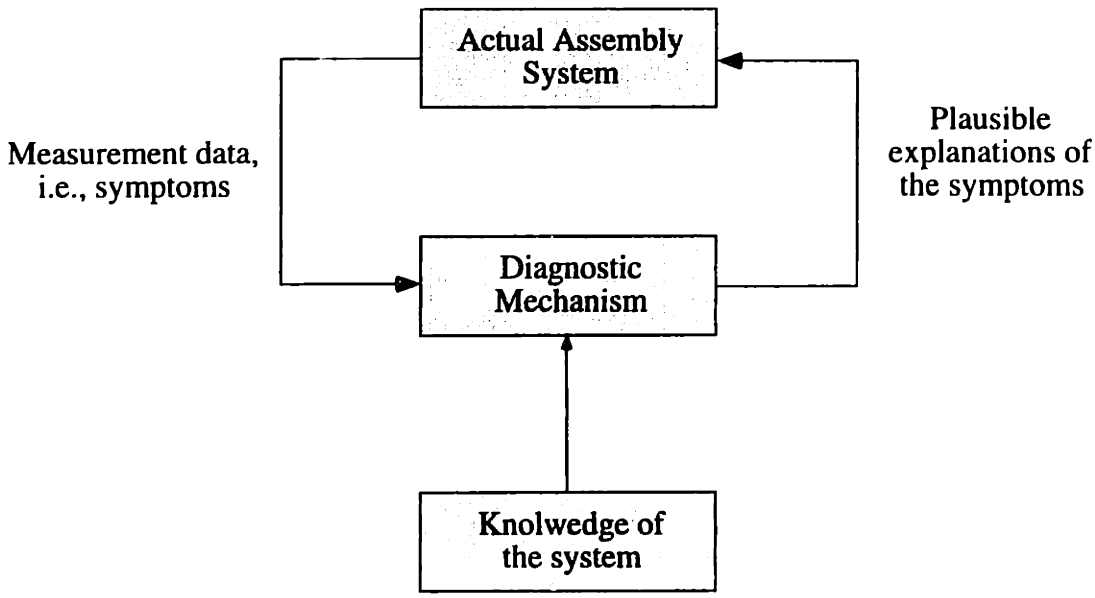

Figure 6.9 Schematic of the diagnostic problem solving process

6.3.2. Inherent difficulties of diagnosis

Diagnosing assembly problems is difficult because of the following reasons.

- The system is very complex and thus no one in the organization has knowledge of the entire system.

- Measurement is essential for diagnosis; however, only a limited number of points are measurable due to both technical and economical reasons, e.g., measuring device cannot reach certain points or it is impractical to measure every single point on the vehicle.

- Even if the system is normal, measurement data are never identical to their nominal values but vary around the nominal because of inherent variations in the manufacturing and assembly process. These inherent variations contaminate the symptoms making diagnosis difficult.

- Sometimes multiple dimensions are faulty simultaneously. Multiple faults mix their symptoms making diagnosis even more difficult.

The object of this chapter is to propose a computational method to guide the diagnosis process from (1) knowledge of the system and (2) measurement data.

6.4. Representation of system knowledge

The relations between the measuring points and the critical dimensions listed in table 6.1 can be rewritten in the form

$$\begin{Bmatrix} \Delta m_1 \\ \Delta m_2 \\ \vdots \\ \Delta m_M \end{Bmatrix} = \begin{bmatrix} & & & \\ \mathbf{d}_1 & \mathbf{d}_2 & \cdots & \mathbf{d}_N \\ & & & \end{bmatrix} \begin{Bmatrix} \Delta c_1 \\ \Delta c_2 \\ \vdots \\ \Delta c_N \end{Bmatrix} \qquad \text{Eq. 6.1}$$

where Δm_i is the deviation of the $i-th$ measuring points, Δc_i is the deviation of the $i-th$ critical dimension, and $\mathbf{d}_i$ is the deviation of measuring points for a unit perturbation in the $i-th$ critical dimension, i.e., the $i-th$ deviation mode. Or simply,

$$\Delta \mathbf{m} = \mathbf{D}\Delta \mathbf{c} \qquad \text{Eq. 6.2}$$

where $\Delta\mathbf{m}$ is the column vector of Δm_i's, $\mathbf{D}$ is a matrix consists of column vectors $\mathbf{d}_i$'s, and $\Delta\mathbf{c}$ is the column vector of Δc_i's.

In Eq. 6.1, ideally $\Delta\mathbf{m}$ and $\Delta\mathbf{c}$ should be zero vectors. In reality, however, $\Delta\mathbf{c}$ have variations, and therefore, $\Delta\mathbf{m}$ have variations. If $\Delta\mathbf{m}$ is within tolerance, the system is within control, otherwise the system is out of control. Diagnosis is the process of finding the cause(s) when the system is out of control. In other words, diagnosis is solving the equation

$$\Delta\tilde{\mathbf{m}} = \mathbf{D}\Delta\mathbf{c} \qquad \text{Eq. 6.3}$$

where $\Delta\tilde{\mathbf{m}}$ is the given measurement data.

6.5. Diagnostic mechanism: for special cases

If the number of measuring points is equal to that of the critical dimensions, i.e., $M = N$ in Eq. 6.1, and the $\mathbf{d}_i$'s are linearly independent, then $\Delta\mathbf{c}$ is simply

$$\Delta\mathbf{c} = \mathbf{D}^{-1}\Delta\tilde{\mathbf{m}}. \qquad \text{Eq. 6.4}$$

Thus, we can say that non-zero Δc_i's are the cause of $\Delta\tilde{\mathbf{m}}$.

If $M > N$, and the $\mathbf{d}_i$'s are linearly independent, then the least square solution of Eq 6.3 is

$$\Delta\hat{\mathbf{c}} = \left(\mathbf{D}^T\mathbf{D}\right)^{-1}\mathbf{D}^T\Delta\tilde{\mathbf{m}} \qquad \text{Eq. 6.5}$$

with the residual error[3]

$$\mathbf{e} \equiv \Delta\tilde{\mathbf{m}} - \mathbf{D}\Delta\hat{\mathbf{c}} = \Delta\tilde{\mathbf{m}} - \mathbf{D}\left(\mathbf{D}^T\mathbf{D}\right)^{-1}\mathbf{D}^T\Delta\tilde{\mathbf{m}}. \qquad \text{Eq. 6.6}$$

---

[3]The residual error results from the difference between the actual system and the assembly model as well as from the measuring errors. The residual error should be small if the assembly model is accurate.

In the above two cases, finding the cause(s) of $\Delta\tilde{\mathbf{m}}$ is straightforward. Very often, however, the number of measuring points is much smaller than the number of critical dimensions, i.e., $M \leq N$. When $M \leq N$, there exist, in general, an infinite number of solutions to Eq. 6.3. Although finding the exact cause(s) is impossible in such cases, we can still extract some useful information to guide the diagnostic process.

6.6. Diagnostic mechanism: for a single fault

Let us assume that it is not very likely that multiple dimensions are faulty simultaneously. Qualitatively speaking, if the problem at hand is caused by a single faulty dimension, the deviation of measuring points should resemble the deviation mode of the faulty dimension. This resemblance is indicated by a coefficient[4]:

$$r_k = \frac{\sum_{i=1}^{i=M} \left(\Delta\tilde{m}_i \cdot d_{i,k}\right)}{\sqrt{\sum_{i=1}^{i=M} \Delta\tilde{m}_i^2} \sqrt{\sum_{i=1}^{i=M} d_{i,k}^2}} \qquad \text{Eq. 6.7}$$

where $\Delta\tilde{m}_i$ is the $i-th$ element of the given measurement data $\Delta\tilde{\mathbf{m}}$, and $d_{i,k}$ is the $i-th$ element of the $k-th$ deviation mode $\mathbf{d}_k$. Thus, we can say that the critical dimension, whose deviation mode has the largest coefficient given in Eq. 6.7, is the most likely cause of the problem.

The limitation of this approach is that diagnosis fails when multiple dimensions are faulty simultaneously. This is because when multiple dimensions are faulty at the same time, the deviation of measuring points do not necessarily resemble the deviation modes of the faulty dimensions.

---

[4]This coefficient has the same form as the coefficient of correlation between $\Delta\tilde{\mathbf{m}}$ and $\mathbf{d}_k$.

6.7. Diagnostic mechanism: for multiple faults

Now let us consider the case when K dimensions are faulty at the same time where $K < M$. Then, the number of possible causes is given in the formula:

$$\sum_{i=1}^{K} \begin{Bmatrix} N \\ i \end{Bmatrix} \qquad \text{Eq. 6.8}$$

where K is the maximum number of faulty dimensions ($K < M$), and N is the number of critical dimensions. In other words, if up to K dimensions can be faulty at the same time, there are

$$\sum_{i=1}^{K} \begin{Bmatrix} N \\ i \end{Bmatrix}$$

number of candidate explanations.

6.7.1. Qualitative description of the approach

In each candidate explanation, a set of critical dimension(s) is assumed to be faulty, while the rest of critical dimensions are assumed to be not faulty. If this assumption is correct, the given measurement data should be well approximated by a linear combination of deviation modes that correspond to the critical dimensions that are assumed to be faulty. This is illustrated in the following two examples.

Example 6.1 Suppose that four dimensions Δc_1, Δc_2, Δc_3, and Δc_4 are critical to the measuring points, Δm_1, Δm_2, and Δm_3, and their relationships are known to have the form

$$\begin{Bmatrix} \Delta m_1 \\ \Delta m_2 \\ \Delta m_3 \end{Bmatrix} = \begin{bmatrix} 2 & 1 & 0 & 0 \\ 1 & 2 & 2 & 1 \\ 1 & 0 & 1 & 1 \end{bmatrix} \begin{Bmatrix} \Delta c_1 \\ \Delta c_2 \\ \Delta c_3 \\ \Delta c_4 \end{Bmatrix}. \qquad \text{Eq. 6.9}$$

Also suppose that the given measurement data are

$$\begin{Bmatrix} \Delta\tilde{m}_1 \\ \Delta\tilde{m}_2 \\ \Delta\tilde{m}_3 \end{Bmatrix} = \begin{Bmatrix} 0.2 \\ 2.1 \\ 2.2 \end{Bmatrix}, \begin{Bmatrix} 0.1 \\ 1.1 \\ 0.9 \end{Bmatrix}, \begin{Bmatrix} -0.1 \\ 1.5 \\ 1.6 \end{Bmatrix}, \text{ and } \begin{Bmatrix} 0.1 \\ 0.5 \\ 0.6 \end{Bmatrix}.$$

The measurement data and deviation modes are illustrated in Figure 6.10. The three axes correspond to Δm_1, Δm_2, and Δm_3. The lines segments represent deviation modes $\mathbf{d}_1$, $\mathbf{d}_2$, $\mathbf{d}_3$, and $\mathbf{d}_4$. Black dots represent the measurement data points.

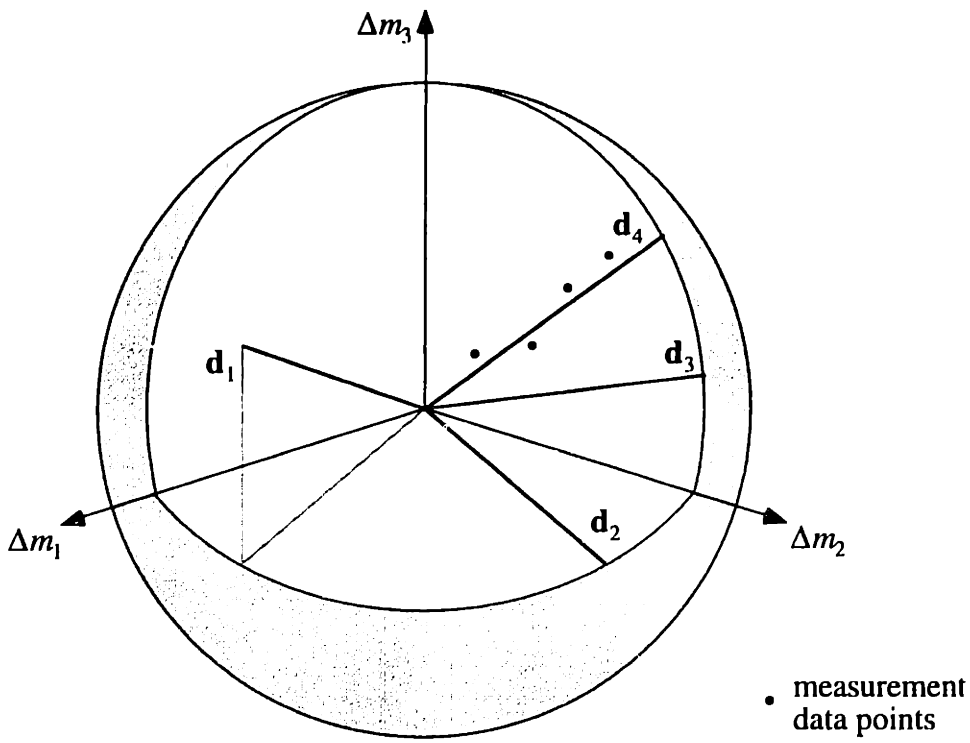

Figure 6.10 Measurement data and deviation modes

Let us test whether the following assumptions are consistent with the measurement data.

Assumption 1: c_1 is faulty while the rest of critical dimensions are not faulty.

Assumption 2: c_2 is faulty while the rest of critical dimensions are not faulty.

Assumption 3: c_3 is faulty while the rest of critical dimensions are not faulty.

Assumption 4: c_4 is faulty while the rest of critical dimensions are not faulty.

Note that in the figure, all the measurement data points are near the line segment that corresponds to $\mathbf{d}_4$. This means that for every measurement data point, there exists a Δc_4 that closely approximates the measurement data. Thus, we can say that assumption 4 is a plausible explanation for the given measurement data $\Delta\tilde{\mathbf{m}}$. On the other hand, the measurement data points are far from the line segments that correspond to $\mathbf{d}_1$, $\mathbf{d}_2$, and $\mathbf{d}_3$. Thus we can say that assumption 1, 2, and 3 are not plausible explanations for the given measurement data $\Delta\tilde{\mathbf{m}}$.

The same analogy can be applied to the cases of multiple faults. Consider the following example.

Example 6.2 Suppose that we have the same relation between $\Delta\mathbf{m}$ and $\Delta\mathbf{c}$ as in Eq. 6.9, but this time measurement data are different as shown in Figure 6.11.

Any assumption in Example 6.1 is not consistent with the measurement data because the given measurement data points are not close to any of the line segments. Let us test whether the following assumptions are consistent with the measurement data.

Assumption 5: c_1 and c_2 are faulty while the rest of critical dimensions are not faulty.

Assumption 6: c_1 and c_3 are faulty while the rest of critical dimensions are not faulty.

Assumption 7: c_1 and c_4 are faulty while the rest of critical dimensions are not faulty.

Assumption 8: c_2 and c_3 are faulty while the rest of critical dimensions are not faulty.

Assumption 9: c_2 and c_4 are faulty while the rest of critical dimensions are not faulty.

Assumption 10: c_3 and c_4 are faulty while the rest of critical dimensions are not faulty.

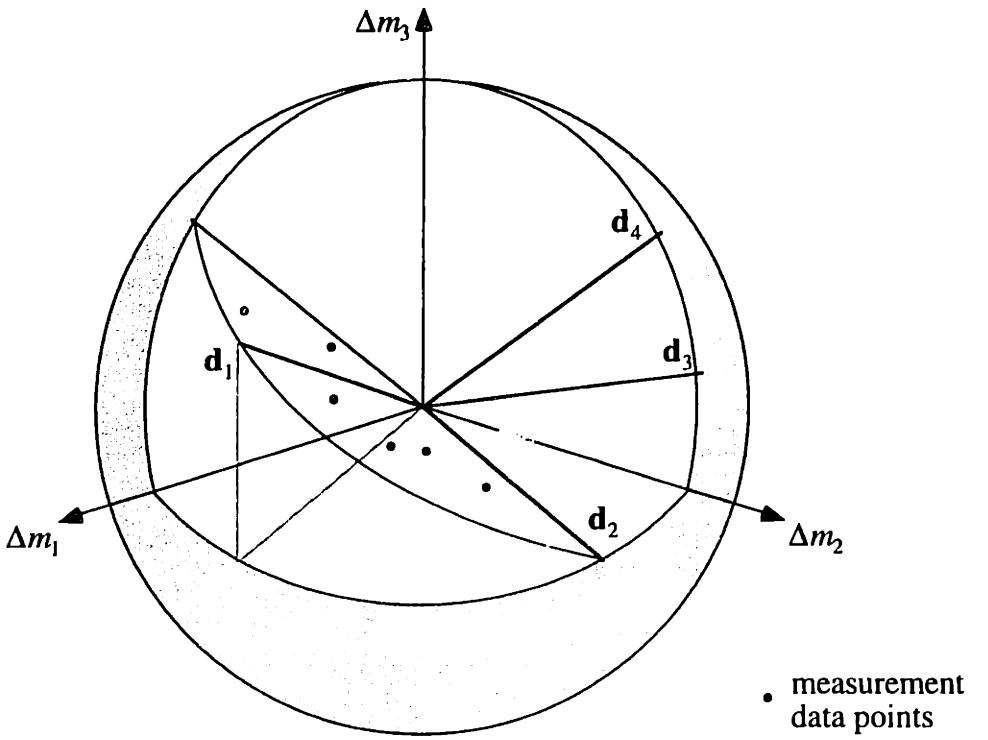

Figure 6.11 Measurement data and a plane constructed by two deviation modes

Note that in the figure, all the measurement data points are near the plane constructed by the line segments correspond to $\mathbf{d}_1$ and $\mathbf{d}_2$. This means that for every measurement data point there exist a Δc_1 and Δc_2 that closely approximate the measurement data. Thus we can say that the assumption 6 is a plausible explanation for the given symptom $\Delta\tilde{\mathbf{m}}$. On the other hand, the measurement data points are far from the planes constructed by the other line segments. Thus we can

say that assumption 6, 7, 8, 9, and 10 are not plausible explanations for the given $\Delta\tilde{\mathbf{m}}$.

6.7.2. Quantitative criteria for plausible explanations

Deciding whether an explanation is plausible or not is a subjective matter. Strict criteria tends to increase the probability that the true cause(s) are rejected in the test, while generous criteria tends to increase the probability that false cause(s) are accepted in the test. This section describes one of the quantitative criteria that has been tested.

Let $\Delta\mathbf{c}^f$ be the sub-vector of $\Delta\mathbf{c}$ that are assumed to be faulty, and also let $\Delta\mathbf{c}^{nf}$ be the a sub-vector of $\Delta\mathbf{c}$ that are assumed to be not faulty. Again, let us assume the dimension of the $\Delta\mathbf{c}^f$ is lower than that of $\Delta\mathbf{m}$, i.e., $K < M$. We can partition Eq 6.2 in the form

$$\Delta\mathbf{m} = \mathbf{D}^f \Delta\mathbf{c}^f + \mathbf{D}^{nf} \Delta\mathbf{c}^{nf} \qquad \text{Eq. 6.10}$$

where $\mathbf{D}^f$ and $\mathbf{D}^{nf}$ are submatrices of $\mathbf{D}$ that correspond to the deviation modes of $\Delta\mathbf{c}^f$ and $\Delta\mathbf{c}^{nf}$, respectively.

Maximum likelihood estimation of $\Delta\mathbf{c}^f$: $\Delta\hat{\mathbf{c}}^f$

The first step is to find the $\Delta\mathbf{c}^f$ that best approximate the given measurement data $\Delta\tilde{\mathbf{m}}$ assuming $\mathbf{D}^{nf}\Delta\mathbf{c}^{nf}$ is small, i.e., assuming that $\Delta\tilde{\mathbf{m}}$ and $\Delta\mathbf{c}^f$ have the following relation.

$$\Delta\tilde{\mathbf{m}} = \mathbf{D}^f \Delta\mathbf{c}^f + \mathbf{e} \qquad \text{Eq. 6.11}$$

where $\mathbf{e}$ is a small unmodeled error vector.

Let $\Delta\hat{\mathbf{c}}^f$ be the maximum likelihood estimation of $\Delta\mathbf{c}^f$. Several methods exist to find $\Delta\hat{\mathbf{c}}^f$: least square fitting, chi-square fitting, etc. [Press 92]. The solution of least square fitting minimizes the quantity,

$$\sum_{i=1}^{M}\left[\Delta\tilde{m}_i - \left(\mathbf{D}^f \Delta\hat{\mathbf{c}}^f\right)_i\right]^2, \qquad \text{Eq. 6.12}$$

while the solution of chi-square fitting minimizes the quantity

$$\sum_{i=1}^{M}\left[\frac{\Delta\tilde{m}_i - \left(\mathbf{D}^f \Delta\hat{\mathbf{c}}^f\right)_i}{\sigma(\mathbf{e}_i)}\right]^2, \qquad \text{Eq. 6.13}$$

where $\sigma(\mathbf{e}_i)$ is the standard deviation of unmodeled error of the $i-th$ measuring point.

Least square fitting is a special case of chi-square fitting, i.e., when $\sigma(\mathbf{e}_i)$ is the same for every measuring point. Because the amount of $\mathbf{e}_i$'s are not usually the same, chi-square fitting is preferred. $\sigma(\mathbf{e}_i)$ in Eq. 6.13 can be estimated from $\mathbf{D}^f \Delta\hat{\mathbf{c}}^f$ in the following way.

Let us define $\mathbf{e}^{nf}$ as

$$\mathbf{e}^{nf} \equiv \mathbf{D}^{nf} \Delta\mathbf{c}^{nf}. \qquad \text{Eq. 6.14}$$

Then $\mathbf{e}$ in Eq 6.11 is a function of $\mathbf{e}^{nf}$ and measuring error. If we neglect measuring error, $\mathbf{e}$ is $\mathbf{e}^{nf}$. If we further assume that Δc_i^{nf}'s are independent and have normal distributions, $\sigma(\mathbf{e}_i)$ can be calculated using the Root Sum Square method[5]:

$$\sigma(\mathbf{e}_i) = \sqrt{\sum_{k=1}^{N-F} (\sigma(\Delta c_k^{nf}) d_{k,i}^{nf})^2} \qquad \text{Eq. 6.15}$$

where Δc_k^{nf} is the $k-th$ element of $\Delta\mathbf{c}^{nf}$, $\sigma(\Delta c_k^{nf})$ is the standard deviation of Δc_k^{nf} which is presumed to be known, $d_{k,i}^{nf}$ is the $i-th$ element of the $k-th$ deviation mode $\mathbf{d}_k$, and $N-F$ is the dimension of vector $\mathbf{c}^{nf}$.

[5]See section 2.3.

Strength of the explanation

Let us define $\mathbf{e}^f$ as

$$\mathbf{e}^f = \Delta\mathbf{m} - \mathbf{D}^f \Delta\hat{\mathbf{c}}^f \qquad \text{Eq 6.16}$$

Then $\mathbf{e}^f$ is the deviation of the actual measurement data in the F dimensional space constructed by $\Delta\mathbf{c}^f$. The distribution of $\mathbf{e}^f$'s is an indicator of the strength of the assumption.

If the assumption that $\Delta\mathbf{c}^f$ is the sub-vector of $\Delta\mathbf{c}$ that are faulty is in fact true, e_i^f should have a distribution with a zero mean and a standard deviation smaller than that of e_i^{nf}. These criteria are compounded in the following form.

$$\sigma'(e_i^f) \le \sigma(e_i^{nf}) \qquad \text{Eq. 6.17}$$

where $\sigma'(e_i^f)$ is the standard deviation of e_i^f's assuming their mean is zero:

$$\sigma'(e_i^f) = \sqrt{\frac{\sum_{k=1}^{n} \left(e_{i,k}^f\right)^2}{n}} \qquad \text{Eq. 6.18}$$

where $e_{i,k}^f$ is the $i-th$ element of the $k-th$ measurement data set, and n is the number of sets of measurement data.

If we assume e_i^f is a chi-distributed random variable, then we can test Eq. 6.17 with the following criteria:

$$\sigma'(e_i^f)^2 \le \frac{\chi^2(\alpha;n)}{n} \sigma(e_i^{nf})^2 \qquad \text{Eq. 6.19}$$

where $\chi^2(\alpha;r)$ is the upper percentage points of the chi-square distribution, and n is the number of sets of measurement data [Hamilton 64].

To summarize, Eq. 6.19 is a criteria for a plausible explanation. e_i^f and e_i^{nf} in Eq. 6.19 can be found from Eq. 6.16 and Eq. 6.14, respectively.

6.7.3. Further refinement of multiple-fault-diagnosis

Consideration on the probability of a certain dimension being faulty

We can use other useful information to further reduce the plausible explanations. For example, it is often known that the probability that a dimension is faulty by more than a certain limit, say, 20 times the standard deviation, is almost zero. It is known from experience that such information is also very useful to reduce the number of plausible explanations.

Search strategies

If $\Delta \mathbf{c}^f$ passes the goodness of explanation test, then it is guaranteed that any combination of critical dimensions that include $\Delta \mathbf{c}^f$ will pass the test. Therefore, if $\Delta \mathbf{c}^f$ passes the strength of explanation test, there is no need to pursue the tests for any combination of critical dimensions that includes $\Delta \mathbf{c}^f$. This reduces the computation time drastically.

6.8. Validation

Assembly Model

Results of section 6.1 are used for validation of the diagnostic mechanism proposed in section 6.6. The deviation mode matrix is generated from Table 6.1.

Test set up

Ten sets of measurement data are randomly generated assuming that all critical dimensions have a normal distribution and the means of the second and nineteenth critical dimensions are shifted by 1.5 mm and 0.5 degree receptively while the rest of critical dimensions are

ideal. Standard deviations of location and orientation errors are assumed to be 0.2 mm and 0.1 degree, respectively. The sample generated data are:

	m_1(x)	m_2(x)	m_3(y)	m_4(y)	m_5(y)	m_6(y)
set 1	0.02	1.90	2.86	2.22	1.73	0.97
set 2	-0.40	2.08	4.16	2.62	2.00	0.95
set 3	-0.39	0.12	2.42	2.63	1.94	-0.03
set 4	0.13	0.85	2.43	2.11	1.70	0.61
set 5	0.53	0.31	2.31	1.85	1.91	0.25
set 6	0.30	3.96	1.73	2.19	1.11	0.81
set 7	0.37	2.01	3.42	2.63	2.51	1.14
set 8	0.03	1.11	2.51	3.27	1.49	0.73
set 9	0.93	2.66	2.39	2.10	1.44	-0.59
set 10	0.15	3.01	2.55	2.12	1.66	0.47

Table 6.2 Measurement data

Results

K in Eq. 6.9, i.e., the maximum number of dimensions can be faulty simultaneously, is chosen to be 3. α in Eq. 6.19 is chosen to be 0.05 which corresponds to 5% Type 1 error[6]. The diagnostic mechanism described in section 6.6 provided the explanations in Table 6.2.

[6]Type I error is rejection of a true hypothesis [Hamilton 64]

Explanation 1	c_2 and c_{19} are faulty
Explanation 2	c_4 and c_{19} are faulty
Explanation 3	c_9 and c_{19} are faulty
Explanation 4	c_2, c_{12}, and c_{19} are faulty
Explanation 5	c_4, c_{12}, and c_{19} are faulty
Explanation 6	c_9, c_{12}, and c_{19} are faulty

Table 6.2 Diagnosis results (c_i means the i-th critical dimension in Table 6.1)

Discussion

Because there are nineteen critical dimensions and K is chosen to be three, there are

$$\sum_{i=1}^{2}\left\{\begin{matrix}19\\ i\end{matrix}\right\} = 19 + \frac{19\times 18}{2\times 1} + \frac{19\times 18\times 17}{3\times 2\times 1} = 1159$$

possible explanations for any measurement data. The proposed diagnostic mechanism found the six most plausible explanations for the given measurement data. The true cause is identified in the first explanation in Table 6.2; the second and the nineteenth critical dimensions are faulty. Five other explanations are provided which are not the causes on which the measurement data generated is based. This is natural because linear combination of their deviations modes approximate any linear combination of deviation modes of c_2 and c_{19}, i.e., their deviation modes span the same vector space.

The test is run with many other measurement data sets that are generated assuming various combinations of critical dimensions are faulty in various ways, i.e., both mean shift and large variance. The following are the observations on the test results.

- In general, proposed diagnostic mechanism works better when the number of faulty critical dimensions is small.

- It works better when faulty dimensions are faulty distinctively.

- The diagnostic mechanism is sensitive to α in Eq. 6.19. Larger α tend to increase the probability that the true cause is rejected in the test, i.e., Type I error, while smaller α tend to increase the probability that a false cause is accepted in the test, i.e., Type II error.

7

Conclusion

7.1. Contributions

This thesis has addressed the problems of

- representing and modeling the assembly of compliant, non-ideal parts
- simulating the propagation of variations in assembly
- exploiting the assembly model for identification of critical dimensions, evaluation of robustness of design to variations, and diagnosis of variation-related assembly problems.

Several new concepts are proposed to represent assemblies of compliant, non-ideal parts in Computer-aided design systems:

- PCFR cycles: The assembly process is represented as a series of PCFR cycles consisting of four steps: Place, Clamp, Fasten, and Release.
- Contact chains: Methods to represent interaction between parts and tooling are developed. Contact chains keep track of contact states at each step of PCFR cycles.

- Displacement vectors: A mathematical framework is developed that collectively describes the relations between variations in parts and tooling, part displacements and deformations, and spatial relationships between mating features.

The following work is presented in this thesis:

- A computational framework was established to simulate the propagation of variations in the assembly of compliant parts.
- An experimental software implementation is developed and tested for simple two dimensional assemblies.
- Computational methods are developed and implemented for the diagnosis of variation-related assembly problems using the proposed assembly model.

Major findings in this work are:

- Variations due to part deformations during assembly are as large and cannot be neglected.
- Variations in assembly tooling are as critical as variations in incoming parts.

7.2. Recommendations

7.2.1. Other applications of the assembly model

It would be straightforward to conduct tolerance analysis based on the assembly model proposed in this thesis for verification of tolerance specifications during design. The difficult part of the problem is to predict variations in manufactured parts and tooling before parts and tooling are manufactured. It would be a challenging research topic to develop a model to predict variations in manufactured parts.

7.2.2. Limitations and Possible Improvements

Some limitations of the work are discussed below along with improvements and extensions that could be made.

Currently, the proposed assembly is implemented and tested in two dimensions. The next immediate step is to implement and test the model in three dimensions.

The current representation method represents only position errors. Generalizing the model to accommodate other types of variations, such as shape and size errors, would be a challenging research topic.

In this thesis, a simplified model of the physical phenomena is used. More accurate estimation can be obtained by including the following in the model: contact forces at other than mating features, friction forces, thermal effects during welding, etc. Trade-off's need to be made between the accuracy of estimation and the required time for modeling and computation.

This thesis does not cover position uncertainties. Position uncertainties refer to cases where part positions are not uniquely defined but instead there exist a range of possible positions. To obtain a more accurate estimation, position uncertainties need to be included in the model.

References

Variation Systems Analysis, Inc. (VSA), Marketing brochure, 300 Maple Park Boulevard S. Clair Shores, Michigan 48091-3771, 1995.

The American National Standard ANSI Y14.5-1982, "Dimensioning and tolerancing for engineering drawings," American National Standards Institute, New York City.

Ambler, A. P., and Popplestone, R. J., "Inferring the positions of bodies from specified spatial relations," Artificial Intelligence, Vol. 6, 1975.

Bathe, K., J., "Finite element procedures in engineering analysis," Prentice-Hall Inc., New Jersey, 1982.

Bjorke, O., "Computer-aided tolerancing," second edition, ASME Press, New York, 1989.

Ceglarek, D., Shi, J., and Wu, S. M., "A knowledge-based diagnostic approach for the launch of the auto-body assembly process," Journal of Engineering for Industry, Vol. 116, November 1994.

Chase, K. W. and Parkinson, A. R., "A survey of research in the application of tolerance analysis to the design of mechanical assemblies," Research in Engineering Design, Vol. 3, 1991.

Crandall, S. et al, "An introduction to the mechanics of solids - 2nd edition," McGraw-Hill Inc., 1978.

Crandall, S. et al, "Dynamics of mechanical and electromechanical systems," Krieger Publishing Company, Florida, 1968.

Fleming, A., "Geometric relationships between toleranced features," Artificial Intelligence 37, 1988.

Fortini, E. T., "Dimensioning for interchangeable manufacture," Industrial Press Inc., New York, 1967.

Gossard, D., "Bridging the gap between design and manufacturing - The Role of Tolerances and Features," Proceedings of Seagrant Conference, Cambridge, MA, October 1988.

Hamilton, W. C., "Statistics in physical science - Estimation, Hypothesis testing, and Least Squares," The Roland Press Company, New York, 1964.

Hillyard, R. C. and Braid, I. C., "Analysis of dimensions and tolerances in computer aided mechanical design," Computer Aided Design, Vol. 10, No. 3, May 1978.

Hoffman, P., "Analysis of tolerances and process inaccuracies in discrete part manufacturing," Computer-aided Design, Vol. 14, No. 2, March 1982.

Hogg, R. V. and Ledolter, J., "Applied statics for engineers and physical scientists - 2nd edition," Macmillan Publishing Company, New York, 1987.

Hu, S. J. and Wu, S. M., "Identifying sources of variation in automobile body assembly using principal component analysis," Transaction of NAMRI/SME, Volume XX, 1992.

Inui, M. and Kimura, F., "Algebraic reasoning of position uncertainties of parts in an assembly," ACM, 1991.

Juster, N. P., "Modelling and representation of dimensions and tolerances: a Survey," Computer-aided Design, Vol. 24, No. 1, January 1992.

Kardestuncer, H., "Elementary matrix analysis of structures," McGraw-Hill Inc., New York, 1974.

Lee, K. and Andrews, G., "Inference of the positions of components in an assembly: Part 2," Computer-aided Design, Vol. 17, No. 1, January/February 1985.

Light, R. A. and Gossard, D. C., "Modification of geometric models through variational geometry," Computer-aided Design, Vol. 4, No. 4, 1982.

Martin, H. C., "Introduction to matrix methods of structural analysis," McGraw-Hill Inc., 1966.

Mortenson, M. E., "Geometric modeling," John Wiley & Sons, Inc., New York, 1985.

Nigam, S. D. and Turner, J. U., "Review of statistical approaches to tolerance analysis," Computer-aided Design, Vol. 27, No. 1, 1995.

Pau, L. F., "Failure diagnosis and performance monitoring," Marcel Dekker Inc., New York, 1981.

Paul, R. P., "Robot manipulators: mathematics, programming, and control," The MIT Press, Cambridge, Massachusetts, 1981.

Press, W. H. et al, "Numerical recipes in C - 2nd edition," Cambridge University Press, New York, 1992.

Reddy, J. N., "An introduction to the finite element method - 2nd edition, "McGraw-Hill Inc., New Jersey, 1993.

Requicha, A., "Toward a theory of geometric tolerancing," The International Journal of Robotics Research, Vol. 2, No. 4, Winter 1983.

Rocheleau, D. N. and Lee, K., "System for interactive assembly modelling," Computer-aided Design, Vo. 19, No. 2, 1987.

Roodvoets, S. C., "An evaluation of the influence of platform team organization on product development performance," M.S. Thesis, Massachusetts Institute of Technology, 1991.

Roy, U., Liu, C. R., and Woo, T. C., "Review of dimensioning and tolerancing: representation and processing," Computer-aided Design, Vol. 23, No. 7, September 1991.

Shimada, K., "Physically-based mesh generation: automated triangulation of surfaces and volumes via bubble packing," Ph.D. dissertation, MIT, 1993.

Srinivasan, V. and Jayaraman, R., " Geometrical tolerancing 1: Virtual boundary requirements," IBM Journal or Research and Development, Vol. 33, No. 2, 1989.

Srinivasan, V. and Jayaraman, R., " Geometrical tolerancing 2: Conditional tolerances," IBM Journal or Research and Development, Vol. 33, No. 2, 1989.

Taguchi, G. et al., "Quality engineering in production systems," McGraw-Hill, 1989.

Turner, J. U., "Tolerances in computer-aided geometric design," Ph.D. Thesis, Rensselaer Polytechnic Institute, 1987.

Turner, J. U., "Relative positioning of parts in assemblies using mathematical programming," Computer-aided Design, Vol. 22, No. 7, September 1990.

Turner, J. U., "Relative position of variational part models for design analysis," Computer-aided Design, Vo. 26, No. 5, May 1994.

Turner, J. U., "Review of statistical approaches to tolerance analysis," Computer-aided Design, Vo. 27, No. 1, 1995.

Appendix A
Homogeneous Transformation Matrix

Homogeneous transformation matrix is a 4×4 matrix that represents translation, rotation, and scaling (or stretching) of a vector. Homogeneous transformation matrix corresponding to translation and rotation is written in a form

$$\mathbf{T}=\left[\begin{array}{ccc|c} & \mathbf{R} & & \mathbf{t} \\ \hline 0 & 0 & 0 & 1 \end{array}\right] \qquad \text{Eq. A.1}$$

where $\mathbf{R}$ is a 3×3 matrix corresponding to the rotation of the coordinate frame, and $\mathbf{t}$ is a 3×1 vector corresponding to the translation of the coordinate frame.

There are many ways to represent the rotation matrix $\mathbf{R}$ [Paul 81]. One way of representing the rotation is using roll, pitch, and yaw: roll corresponds to a rotation ϕ about the z-axis, pitch corresponds to a rotation θ about the y-axis, and yaw corresponds to a rotation ψ about the x-axis. The order of rotation with respect to the reference coordinate system is specified as

$$RPY(\phi,\theta,\psi) = Rot(z,\phi)Rot(y,\theta)Rot(x,\psi)$$

which is a rotation ψ about the x-axis, followed by a rotation θ about the y-axis, and finally a rotation ϕ about the z-axis. Therefore, the entire rotation can be written as

$$\mathbf{R}=\begin{bmatrix} c_\phi c_\theta & c_\phi s_\theta s_\psi - s_\phi c_\psi & c_\phi s_\theta c_\psi + s_\phi s_\psi \\ s_\phi c_\theta & s_\phi s_\theta s_\psi + c_\phi c_\psi & s_\phi s_\theta c_\psi - c_\phi s_\psi \\ -s_\theta & c_\theta s_\psi & c_\theta c_\psi \end{bmatrix}. \qquad \text{Eq. A.2}$$

where $c_\alpha \equiv \cos(\alpha)$ and $s_\alpha \equiv \sin(\alpha)$.

The translation vector $\mathbf{t}$ can be represented as

$$\mathbf{t} = \begin{Bmatrix} x \\ y \\ z \end{Bmatrix} \qquad \text{Eq. A.3}$$

where x, y, and z are the translations along the x, y, and z direction, respectively.

From Eq.'s A.1, A.2, and A.3, the entire transformation given both translation and rotation may be written as

$$\mathbf{T} = \begin{bmatrix} c_\phi c_\theta & c_\phi s_\theta s_\psi - s_\phi c_\psi & c_\phi s_\theta c_\psi + s_\phi s_\psi & x \\ s_\phi c_\theta & s_\phi s_\theta s_\psi + c_\phi c_\psi & s_\phi s_\theta c_\psi - c_\phi s_\psi & y \\ -s_\theta & c_\theta s_\psi & c_\theta c_\psi & z \\ 0 & 0 & 0 & 1 \end{bmatrix}, \qquad \text{Eq. A.4}$$

where $c_\alpha \equiv \cos(\alpha)$ and $s_\alpha \equiv \sin(\alpha)$.

Appendix B
Coordinate Transformation of Displacement Vectors

Displacement vectors defined in two different coordinate frames can be related with the rotation matrix between the coordinate frames. Let ${}^{\mathcal{F}}\varepsilon$ and ${}^{\mathcal{G}}\varepsilon$ be the same displacement vector defined with respect to the coordinate frame $\mathcal{F}$ and $\mathcal{G}$, respectively. Let ${}^{\mathcal{F}}\varepsilon_t$ and ${}^{\mathcal{G}}\varepsilon_t$ be the sub-vectors of ${}^{\mathcal{F}}\varepsilon$ and ${}^{\mathcal{G}}\varepsilon$ that correspond to translation, and also let ${}^{\mathcal{F}}\varepsilon_r$ and ${}^{\mathcal{G}}\varepsilon_r$ be the sub-vectors of ${}^{\mathcal{F}}\varepsilon$ and ${}^{\mathcal{G}}\varepsilon$ that correspond to rotation. Then, ${}^{\mathcal{F}}\varepsilon$ and ${}^{\mathcal{G}}\varepsilon$ are related as in Eq. B.1.

$$\left.\begin{aligned} {}^{\mathcal{F}}\varepsilon_t &= \mathbf{R}\times{}^{\mathcal{G}}\varepsilon_t \\ {}^{\mathcal{F}}\varepsilon_r &= \mathbf{R}\times{}^{\mathcal{G}}\varepsilon_r \end{aligned}\right\} \qquad \text{Eq. B.1}$$

where $\mathbf{R}$ is the rotation matrix that relates the coordinate frame $\mathcal{F}$ and $\mathcal{G}$.

Eq. B.1 can be rewritten as

$${}^{\mathcal{F}}\varepsilon = [\ \mathbf{R}\ |\ \mathbf{R}\ ]{}^{\mathcal{G}}\varepsilon. \qquad \text{Eq. B.2}$$

Appendix C
Shape Error versus Position Error

Shape errors of features in assembly tooling, e.g., locator pins and clamps, are very small compared to position errors. This is because the shape of locator pins and clamps is determined by a single relatively accurate manufacture process, e.g., machining, while the position of locator pins and clamps is affected by many parts and linkages in assembly tooling that supports the pins and clamps.

Shape errors of small features in sheet metal panels, e.g., holes and clamping surfaces, are also very small compared to position errors. Sheet metal panels of automobile bodies are manufactured by the stamping process. A typical stamping process consists of three steps: draw, pierce and trim, and flange. First, draw dies form the basic shape of parts, pierce and trim dies pierce holes and cut trim areas, then flange dies form the detail shape of parts.

Shape errors of holes are negligible

The errors in the size of holes arise mostly during the piercing process while the errors in position of holes arise during almost every step of the stamping process. Piercing is a relatively simple and accurate process compared to the draw and flange processes which lead to complex mechanical material behavior such as plastic deformation and spring back. Under current stamping technology, shape errors and position errors have the order of magnitude difference; diameter of holes normally varies less than ± 0.05 mm, while

position of holes may vary as much as a few millimeters. Therefore, we can say that variations in diameter of holes are negligible compared to position errors.

Shape errors of clamping surfaces and welding surfaces are negligible

In sheet metal parts, position errors of small surface features, e.g., clamping surface, welding surface, etc., are often much bigger than shape errors. Shape errors of a surface feature are affected by local defects such as wrinkles and dimples within the features, while position errors are affected by global defects such as spring back. In most stamped parts, the errors due to local defects are very small compared to the errors due to global defects.

Appendix D
Static Condensation

The following material is based on the book "Finite element procedures in engineering analysis" by Bathe [Bathe 82].

The constitutive $\mathbf{f} = \mathbf{K}\mathbf{u}$ can be partitioned into the form

$$\begin{bmatrix} \mathbf{f}_a \\ \mathbf{f}_c \end{bmatrix} = \begin{bmatrix} \mathbf{K}_{aa} & \mathbf{K}_{ca} \\ \mathbf{K}_{ac} & \mathbf{K}_{cc} \end{bmatrix} \begin{bmatrix} \mathbf{u}_a \\ \mathbf{u}_c \end{bmatrix} \qquad \text{Eq. D.1}$$

where $\mathbf{u}_a$ and $\mathbf{u}_c$ are the vectors of displacements to be retained and condensed out, respectively. The matrices $\mathbf{K}_{aa}$, $\mathbf{K}_{ac}$, $\mathbf{K}_{ca}$ and $\mathbf{K}_{cc}$, and vectors $\mathbf{f}_a$ and $\mathbf{f}_c$ correspond to the displacement vectors $\mathbf{u}_a$ and $\mathbf{u}_c$.

We can rewrite the first equation in Eq. D.1 in the form

$$\mathbf{u}_c = (-\mathbf{K}_{cc}^{-1}\mathbf{K}_{ca})\mathbf{u}_a + \mathbf{K}_{cc}^{-1}\mathbf{f}_c. \qquad \text{Eq. D.2}$$

By substituting Eq. D.2 in the second equation of Eq. D.1, we have

$$\mathbf{f}_a = (\mathbf{K}_{aa} - \mathbf{K}_{ac}\mathbf{K}_{cc}^{-1}\mathbf{K}_{ca})\mathbf{u}_a + \mathbf{K}_{ac}\mathbf{K}_{cc}^{-1}\mathbf{f}_c. \qquad \text{Eq. D.3}$$

Appendix E
Addition of Variations and Displacement

When ϕ, θ, and ψ are small Eq. A.4 can be approximated as

$$\mathbf{T} \approx \begin{bmatrix} 1 & -\phi & \theta & x \\ \phi & 1 & -\psi & y \\ -\theta & \psi & 1 & z \\ 0 & 0 & 0 & 1 \end{bmatrix}. \qquad \text{Eq. E.1}$$

Let $\mathbf{T}(\varepsilon_1)$ and $\mathbf{T}(\varepsilon_2)$ be the homogeneous transformation matrices that correspond to displacement vectors ε_1 and ε_2, respectively. Because ε_1 and ε_2 are small, $\mathbf{T}(\varepsilon_1)$ and $\mathbf{T}(\varepsilon_2)$ are approximately

$$\mathbf{T}(\varepsilon_1) \approx \begin{bmatrix} 1 & -\phi_1 & \theta_1 & x_1 \\ \phi_1 & 1 & -\psi_1 & y_1 \\ -\theta_1 & \psi_1 & 1 & z_1 \\ 0 & 0 & 0 & 1 \end{bmatrix}, \text{ and}$$

$$\mathbf{T}(\varepsilon_2) \approx \begin{bmatrix} 1 & -\phi_2 & \theta_2 & x_1 \\ \phi_2 & 1 & -\psi_2 & y_1 \\ -\theta_2 & \psi_2 & 1 & z_1 \\ 0 & 0 & 0 & 1 \end{bmatrix}. \qquad \text{Eq. E.2}$$

Then, we can say that

$$\mathbf{T}(\varepsilon_1)\mathbf{T}(\varepsilon_2) \approx \mathbf{T}(\varepsilon_2)\mathbf{T}(\varepsilon_1)$$

$$\approx \begin{bmatrix} 1 & -(\phi_1+\phi_2) & \theta_1+\theta_2 & x_1+x_2 \\ \phi_1+\phi_2 & 1 & -(\psi_1+\psi_2) & y_1+y_2 \\ -(\theta_1+\theta_2) & \psi_1+\psi_2 & 1 & z_1+z_2 \\ 0 & 0 & 0 & 1 \end{bmatrix} \quad \text{Eq. E.3}$$

which means that the total displacement of a feature resulting from a displacement after another is independent of the order in which displacements occur. Furthermore, two consecutive transformations $\mathbf{T}(\varepsilon_1)$ and $\mathbf{T}(\varepsilon_2)$ are the same as a singe transformation designated by the sum of error vector ε_1 and ε_2, i.e., $\mathbf{T}(\varepsilon_1+\varepsilon_2)$. This is shown in Eq. E.4.

$$\mathbf{T}(\varepsilon_1)\mathbf{T}(\varepsilon_2)=\mathbf{T}(\varepsilon_2)\mathbf{T}(\varepsilon_1)=\mathbf{T}(\varepsilon_1+\varepsilon_2) \quad \text{Eq. E.4}$$

Thus, we can say that small displacements can be compounded by vector addition.